



NRL/MR/7322--18-9755

## **A Cost-Benefit Analysis of SWAN with Source Term Package ST6**

K.L. EDWARDS

W.E. ROGERS

*Ocean Dynamics and Prediction Branch  
Oceanography Division*

S. SIQUEIRA

*Vencore*

*Stennis Space Center, Mississippi*

P. GAY

K. WOOD

*Naval Oceanographic Office  
Stennis Space Center, Mississippi*

August 10, 2018

Approved for public release; distribution is unlimited.

# REPORT DOCUMENTATION PAGE

*Form Approved*  
*OMB No. 0704-0188*

Public reporting burden for this collection of information is estimated to average 1 hour per response, including the time for reviewing instructions, searching existing data sources, gathering and maintaining the data needed, and completing and reviewing this collection of information. Send comments regarding this burden estimate or any other aspect of this collection of information, including suggestions for reducing this burden to Department of Defense, Washington Headquarters Services, Directorate for Information Operations and Reports (0704-0188), 1215 Jefferson Davis Highway, Suite 1204, Arlington, VA 22202-4302. Respondents should be aware that notwithstanding any other provision of law, no person shall be subject to any penalty for failing to comply with a collection of information if it does not display a currently valid OMB control number. **PLEASE DO NOT RETURN YOUR FORM TO THE ABOVE ADDRESS.**

<b>1. REPORT DATE (DD-MM-YYYY)</b> 10-08-2018			<b>2. REPORT TYPE</b> Memorandum Report		<b>3. DATES COVERED (From - To)</b>	
<b>4. TITLE AND SUBTITLE</b>  A Cost-Benefit Analysis of SWAN with Source Term Package ST60603207N					<b>5a. CONTRACT NUMBER</b>	
					<b>5b. GRANT NUMBER</b>	
					<b>5c. PROGRAM ELEMENT NUMBER</b> 0603207N	
<b>6. AUTHOR(S)</b>  K.L. Edwards, S. Siqueira, W.E. Rogers, P. Gay and K. Wood					<b>5d. PROJECT NUMBER</b>	
					<b>5e. TASK NUMBER</b>	
					<b>5f. WORK UNIT NUMBER</b> 3-5097-C5-5	
<b>7. PERFORMING ORGANIZATION NAME(S) AND ADDRESS(ES)</b>  Naval Research Laboratory Oceanography Division Stennis Space Center, MS 39529-5004					<b>8. PERFORMING ORGANIZATION REPORT NUMBER</b>  NRL/MR/7320--18-9755	
<b>9. SPONSORING / MONITORING AGENCY NAME(S) AND ADDRESS(ES)</b>  Space & Naval Warfare Systems Command 2451 Crystal Drive Arlington, VA 22245-5200					<b>10. SPONSOR / MONITOR'S ACRONYM(S)</b>  SPAWAR	
					<b>11. SPONSOR / MONITOR'S REPORT NUMBER(S)</b>	
<b>12. DISTRIBUTION / AVAILABILITY STATEMENT</b>  Approved for public release; distribution is unlimited.						
<b>13. SUPPLEMENTARY NOTES</b>						
<b>14. ABSTRACT</b>  Simulating WAVes Nearshore (SWAN) is a phase-averaged spectral model used by the U.S. Navy for forecasting waves. Changes to the source term package improve skill within the higher frequencies of the wave energy spectrum, where previous source terms result in non-physical responses to changes in wind speed and the presence of swell. We apply the model to three geographic locations, compare results to buoy data, and show the improved skill in predicting high frequency wave energy for cases when swell is a component of the wave field.						
<b>15. SUBJECT TERMS</b>  Wave Model, SWAN, ST1, ST6, Swell						
<b>16. SECURITY CLASSIFICATION OF:</b>			<b>17. LIMITATION OF ABSTRACT</b>	<b>18. NUMBER OF PAGES</b>	<b>19a. NAME OF RESPONSIBLE PERSON</b>	
<b>a. REPORT</b>	<b>b. ABSTRACT</b>	<b>c. THIS PAGE</b>			Kacey Edwards	
Unclassified Unlimited	Unclassified Unlimited	Unclassified Unlimited	Unclassified Unlimited	8	<b>19b. TELEPHONE NUMBER (include area code)</b> (228) 688-5077	

This page intentionally left blank.

# CONTENTS

<b>LIST OF FIGURES</b>	<b>iv</b>
<b>LIST OF TABLES</b>	<b>vi</b>
<b>1 Introduction</b>	<b>1</b>
<b>2 Approach</b>	<b>2</b>
2.1 DATA SOURCES AND QUALITY CONTROL	3
2.1.1 <i>NDBC Buoys</i>	3
2.1.2 <i>Datowell Buoys</i>	3
2.2 COMPARISON PARAMETERS	3
2.3 COMPARISON METRICS	4
2.3.1 <i>Time Series Comparisons</i>	4
2.3.2 <i>Statistical Comparisons</i>	4
2.4 MODEL SETTINGS	5
2.4.1 <i>Frequency Range</i>	5
2.4.2 <i>Computational Details</i>	6
<b>3 Test Cases</b>	<b>6</b>
3.1 GULF OF MEXICO (GOM)	6
3.1.1 <i>Data Collection</i>	6
3.1.2 <i>Model Setup and Execution</i>	6
3.1.3 <i>Data-Model Comparison</i>	7
3.1.4 <i>Discussion</i>	8
3.2 SOUTHERN CALIFORNIA (SOCAL)	8
3.2.1 <i>Data Collection</i>	8
3.2.2 <i>Model Setup and Execution</i>	8
3.2.3 <i>Data-Model Comparison</i>	10
3.2.4 <i>Discussion</i>	10
3.3 HAWAII	11
3.3.1 <i>Data Collection</i>	11
3.3.2 <i>Model Setup and Execution</i>	11
3.3.3 <i>Data-Model Comparison</i>	12
3.3.4 <i>Discussion</i>	12
<b>4 Conclusions</b>	<b>13</b>
<b>5 Recommendations</b>	<b>13</b>
<b>6 Acknowledgments</b>	<b>14</b>
<b>7 REFERENCES</b>	<b>14</b>
<b>8 TABLES</b>	<b>16</b>
<b>9 FIGURES</b>	<b>28</b>

## LIST OF FIGURES

- FIGURE 1. PROVIDED BY BOB JENSEN, U.S. ARMY CORPS OF ENGINEERS. IT INDICATES THAT THE 3-M DISCUS BUOY NEAR MONTEREY, CA (STATION ID 46042) HAS NEGATIVE BIAS (DARK BLUE COLOR) IN HIGHER FREQUENCIES (RIGHT SIDE OF PLOT) COMPARED WITH A NEARBY WAVERIDER BUOY (STATION ID 46114). 28
- FIGURE 2. A LOG-LOG PLOT OF OBSERVED SPECTRA FROM THE 3-M DISCUS BUOY 310 NM SSW OF KODIAK, AK (STATION ID 46066), COLORED BY 10 M WIND SPEED. NOTICE THE SLOPE OF THE SPECTRAL TAIL SLOPE IS RATHER SUSPECT IN THE 0.3 TO 0.485 HZ RANGE, DEVIATING FROM THE EXPECTED  $S(f) \propto f^{-4}$  FUNCTIONAL FORM – STEEPENING TO APPROACH OR EXCEED  $S(f) \propto f^{-5}$ , INDICATING THAT THE PUBLISHED SPECTRA ARE MISSING ENERGY IN THE HIGHER FREQUENCIES ( $> 0.3$  HZ). 29
- FIGURE 3. (TOP) THE SHOWS THE ENERGY OMITTED FOR THE PERIOD OF JULY-AUGUST 2016, BY NAVO'S MODEL LOWER FREQUENCY LIMIT OF 0.05 HZ (GREEN CURVE) AND BY NRL'S MODEL LOWER FREQUENCY LIMIT OF 0.0418 HZ (BLUE CURVE); (BOTTOM) SHOWS THE WAVE FREQUENCY SPECTRA FOR THE JULY-AUGUST 2016 SOUTHERN CALIFORNIA STUDY. 30
- FIGURE 4. (TOP) THE SHOWS THE ENERGY OMITTED FOR THE PERIOD OF JANUARY-FEBRUARY 2017, BY NAVO'S MODEL LOWER FREQUENCY LIMIT OF 0.05 HZ (GREEN CURVE) AND BY NRL'S MODEL LOWER FREQUENCY LIMIT OF 0.0418 HZ (BLUE CURVE); (BOTTOM) SHOWS THE WAVE FREQUENCY SPECTRA FOR THE JANUARY-FEBRUARY 2017 SOUTHERN CALIFORNIA STUDY. THE SWELL EVENTS DURING WHICH THE LARGEST QUANTITIES OF MISSING ENERGY OCCUR ARE CLEARLY VISIBLE. 30
- FIGURE 5. MODEL GRID CONFIGURATION FOR THE GULF OF MEXICO TEST CASE, G1 (RED), G11 (BLUE), G112 (MAGENTA) AND NDBC BUOYS (BLACK DIAMONDS). 31
- FIGURE 6. COMPARISON OF WIND DATA (BLUE) AND WIND INPUT (RED) FOR THE GULF OF MEXICO TEST CASE. WIND SPEED (TOP) AND DIRECTION (BOTTOM) ARE SHOWN FOR THE LOCATION OF BUOY 42012. 31
- FIGURE 7. REGRESSION ANALYSIS OF SIGNIFICANT WAVE HEIGHT (LEFT), MEAN ENERGY PERIOD (MIDDLE), 4TH MOMENT (RIGHT) USING THE ST1 PACKAGE (RED) AND THE ST6 PACKAGE (BLUE) FOR THE GULF OF MEXICO G1 MODEL. 32
- FIGURE 8. REGRESSION ANALYSIS OF SIGNIFICANT WAVE HEIGHT (LEFT), MEAN ENERGY PERIOD (MIDDLE), 4TH MOMENT (RIGHT) USING THE ST1 PACKAGE (RED) AND THE ST6 PACKAGE (BLUE) FOR THE GULF OF MEXICO G11 MODEL. 32
- FIGURE 9. REGRESSION ANALYSIS OF SIGNIFICANT WAVE HEIGHT (LEFT), MEAN ENERGY PERIOD (MIDDLE), 4TH MOMENT (RIGHT) USING THE ST1 PACKAGE (RED) AND THE ST6 PACKAGE (BLUE) FOR THE GULF OF MEXICO G112 MODEL. 33
- FIGURE 10. MODEL GRID CONFIGURATION FOR THE SOUTHERN CALIFORNIA TEST CASE, CAL1 (RED), CAL2 (BLACK), CAL3 (BLUE) AND NDBC (MAGENTA CIRCLES) AND DATAWELL (CYAN TRIANGLES) BUOYS. 34
- FIGURE 11. BATHYMETRY SURFACES FOR SOUTHERN CALIFORNIA MODELS, CAL1 (LEFT), CAL2 (MIDDLE), CAL3 (RIGHT). 34
- FIGURE 12. INPUT (RED) WIND SPEED (TOP PLOT) AND DIRECTION (BOTTOM PLOT) COMPARED TO OBSERVATIONS AT NDBC BUOY 46047 (BLUE) FOR THE SUMMER (TOP HALF) AND WINTER (BOTTOM HALF) SOUTHERN CALIFORNIA SIMULATIONS. 35
- FIGURE 13. REGRESSION ANALYSIS OF SIGNIFICANT WAVE HEIGHT (LEFT), MEAN ENERGY PERIOD (MIDDLE), 4TH MOMENT (RIGHT) USING THE ST1 PACKAGE (RED) AND THE ST6 PACKAGE (BLUE) FOR THE SOUTHERN CALIFORNIA CAL1 MODEL AND NDBC BUOYS FOR THE SUMMER (TOP) AND WINTER (BOTTOM) PERIODS. 36
- FIGURE 14. REGRESSION ANALYSIS OF SIGNIFICANT WAVE HEIGHT (LEFT), MEAN ENERGY PERIOD (MIDDLE), 4TH MOMENT (RIGHT) USING THE ST1 PACKAGE (RED) AND THE ST6 PACKAGE (BLUE) FOR THE SOUTHERN CALIFORNIA CAL1 MODEL AND DATAWELL BUOYS FOR THE SUMMER (TOP) AND WINTER (BOTTOM) PERIODS. 37
- FIGURE 15. REGRESSION ANALYSIS OF SIGNIFICANT WAVE HEIGHT (LEFT), MEAN ENERGY PERIOD (MIDDLE), 4TH MOMENT (RIGHT) USING THE ST1 PACKAGE (RED) AND THE ST6 PACKAGE (BLUE) FOR THE SOUTHERN CALIFORNIA CAL2 MODEL AND NDBC BUOYS FOR SUMMER (TOP) AND WINTER (BOTTOM) PERIODS. 38
- FIGURE 16. REGRESSION ANALYSIS OF SIGNIFICANT WAVE HEIGHT (LEFT), MEAN ENERGY PERIOD (MIDDLE), 4TH MOMENT (RIGHT) USING THE ST1 PACKAGE (RED) AND THE ST6 PACKAGE (BLUE) FOR THE SOUTHERN CALIFORNIA CAL2 MODEL AND DATAWELL BUOYS FOR SUMMER (TOP) AND WINTER (BOTTOM) PERIODS. 39
- FIGURE 17. REGRESSION ANALYSIS OF SIGNIFICANT WAVE HEIGHT (LEFT), MEAN ENERGY PERIOD (MIDDLE), 4TH MOMENT (RIGHT) USING THE ST1 PACKAGE (RED) AND THE ST6 PACKAGE (BLUE) FOR SOUTHERN CALIFORNIA CAL3 MODEL AND DATAWELL BUOYS FOR SUMMER (TOP) AND WINTER (BOTTOM) PERIODS. 40

- FIGURE 18. MODEL GRID CONFIGURATION FOR THE HAWAII TEST CASE, H1 (BLUE) AND H2 (BLACK) AND DATAWELL Buoys (CYAN TRIANGLES). 41
- FIGURE 19. REGRESSION ANALYSIS OF SIGNIFICANT WAVE HEIGHT (LEFT), MEAN ENERGY PERIOD (MIDDLE), 4TH MOMENT (RIGHT) USING THE ST1 PACKAGE (RED) AND THE ST6 PACKAGE (BLUE) FOR THE HAWAII H1 MODEL AND DATAWELL BUOYS FOR SUMMER (TOP) AND WINTER (BOTTOM) PERIODS. 42
- FIGURE 20. REGRESSION ANALYSIS OF SIGNIFICANT WAVE HEIGHT (LEFT), MEAN ENERGY PERIOD (MIDDLE), 4TH MOMENT (RIGHT) USING THE ST1 PACKAGE (RED) AND THE ST6 PACKAGE (BLUE) FOR THE HAWAII H2 MODEL AND DATAWELL BUOYS FOR SUMMER (TOP) AND WINTER (BOTTOM) PERIODS. 43

# LIST OF TABLES

TABLE 1. NDBC BUOY INFORMATION FOR THE GULF OF MEXICO TEST CASE..... 16

TABLE 2. GRID PROPERTIES FOR GULF OF MEXICO TEST CASE, INCLUDING THE NUMBER OF GRID POINTS AND LENGTHS IN X- AND Y-DIRECTIONS, THE HORIZONTAL RESOLUTION, AND THE NUMBER OF MODEL FREQUENCIES AND DIRECTIONS..... 16

TABLE 3. CORRELATION COEFFICIENTS FOR COMPARISONS OF SIGNIFICANT WAVE HEIGHT, MEAN ENERGY PERIOD, AND THE 4TH MOMENT FOR EACH OF THE GULF OF MEXICO MODELS, G1, G11, AND G112, USING ST1 AND ST6 PACKAGES AND ALL GULF OF MEXICO DATA SOURCES..... 17

TABLE 4. SIGNIFICANT WAVE HEIGHT PERFORMANCE METRICS. BIAS, ROOT MEAN SQUARE ERROR (RMSE), NORMALIZED BIAS (NBIAS), AND SCATTER INDEX (SI) FOR MODEL-DATA COMPARISONS OF GULF OF MEXICO MODELS, G1, G11, AND G112. .... 17

TABLE 5. MEAN ENERGY PERIOD PERFORMANCE METRICS. BIAS, ROOT MEAN SQUARE ERROR (RMSE), NORMALIZED BIAS (NBIAS), AND SCATTER INDEX (SI) FOR MODEL-DATA COMPARISONS OF GULF OF MEXICO MODELS, G1, G11, AND G112. .... 17

TABLE 6. FOURTH SPECTRAL MOMENT PERFORMANCE METRICS. BIAS, ROOT MEAN SQUARE ERROR (RMSE), NORMALIZED BIAS (NBIAS), AND SCATTER INDEX (SI) FOR MODEL-DATA COMPARISONS OF GULF OF MEXICO MODELS, G1, G11, AND G112. .... 18

TABLE 7. CORRELATION COEFFICIENTS FOR COMPARISONS OF SIGNIFICANT WAVE HEIGHT, MEAN ENERGY PERIOD, AND THE 4TH MOMENT FOR EACH OF THE GULF OF MEXICO MODELS, G1, G11, AND G112, USING ST1 AND ST6 PACKAGES AND BUOY 42012. .... 18

TABLE 8. NDBC BUOY INFORMATION FOR THE SOUTHERN CALIFORNIA TEST CASE. .... 18

TABLE 9. DATAWELL BUOY INFORMATION FOR THE SOUTHERN CALIFORNIA TEST CASE. .... 19

TABLE 10. GRID PROPERTIES FOR SOUTHERN CALIFORNIA TEST CASE, INCLUDING THE NUMBER OF GRID POINTS AND LENGTHS IN X- AND Y-DIRECTIONS, THE HORIZONTAL RESOLUTION, AND THE NUMBER OF MODEL FREQUENCIES AND DIRECTIONS. .... 19

TABLE 11. CORRELATION COEFFICIENTS FOR COMPARISONS OF SIGNIFICANT WAVE HEIGHT, MEAN ENERGY PERIOD, AND THE 4TH MOMENT FOR EACH OF THE SOUTHERN CALIFORNIA MODELS, CAL1 AND CAL2, USING ST1 AND ST6 PACKAGES AND NDBC BUOYS..... 20

TABLE 12. CORRELATION COEFFICIENTS FOR COMPARISONS OF SIGNIFICANT WAVE HEIGHT, MEAN ENERGY PERIOD, AND THE 4TH MOMENT FOR EACH OF THE SOUTHERN CALIFORNIA MODELS, CAL1, CAL2, AND CAL3 USING ST1 AND ST6 PACKAGES AND DATAWELL BUOYS. .... 20

TABLE 13. BIAS, ROOT MEAN SQUARE ERROR (RMSE), NORMALIZED BIAS (NBIAS), AND SCATTER INDEX (SI) FOR SIGNIFICANT WAVE HEIGHT MODEL-DATA COMPARISONS OF SOUTHERN CALIFORNIA MODELS AND NDBC DATA. .... 21

TABLE 14. BIAS, ROOT MEAN SQUARE ERROR (RMSE), NORMALIZED BIAS (NBIAS), AND SCATTER INDEX (SI) FOR MODEL-DATA COMPARISONS OF MEAN ENERGY PERIOD FOR SOUTHERN CALIFORNIA MODELS AND NDBC DATA. .... 22

TABLE 15. BIAS, ROOT MEAN SQUARE ERROR (RMSE), NORMALIZED BIAS (NBIAS), AND SCATTER INDEX (SI) FOR 4TH MOMENT MODEL-DATA COMPARISONS OF SOUTHERN CALIFORNIA MODELS AND NDBC DATA. .... 23

TABLE 16. BIAS, ROOT MEAN SQUARE ERROR (RMSE), NORMALIZED BIAS (NBIAS), AND SCATTER INDEX (SI) FOR SIGNIFICANT WAVE HEIGHT MODEL-DATA COMPARISONS OF SOUTHERN CALIFORNIA MODELS AND DATAWELL DATA..... 24

TABLE 17. BIAS, ROOT MEAN SQUARE ERROR (RMSE), NORMALIZED BIAS (NBIAS), AND SCATTER INDEX (SI) FOR TOTAL ENERGY MODEL-DATA COMPARISONS OF SOUTHERN CALIFORNIA MODELS AND DATAWELL DATA. .... 25

TABLE 18. BIAS, ROOT MEAN SQUARE ERROR (RMSE), NORMALIZED BIAS (NBIAS), AND SCATTER INDEX (SI) FOR 4TH MOMENT MODEL-DATA COMPARISONS OF SOUTHERN CALIFORNIA MODELS AND DATAWELL DATA. .... 26

TABLE 19. DATAWELL BUOY INFORMATION FOR THE HAWAII TEST CASE. .... 26

TABLE 20. GRID PROPERTIES FOR HAWAII TEST CASE, INCLUDING THE NUMBER OF GRID POINTS AND LENGTHS IN X- AND Y-DIRECTIONS, THE HORIZONTAL RESOLUTION, AND THE NUMBER OF MODEL FREQUENCIES AND DIRECTIONS..... 27

TABLE 21. CORRELATION COEFFICIENTS FOR COMPARISONS OF SIGNIFICANT WAVE HEIGHT, MEAN ENERGY PERIOD, AND THE 4TH MOMENT FOR EACH OF THE HAWAII MODELS, H1 AND H2, USING ST1 AND ST6 PACKAGES AND ALL HAWAII DATA SOURCES FOR THE SUMMER PERIOD. .... 27

TABLE 22. CORRELATION COEFFICIENTS FOR COMPARISONS OF SIGNIFICANT WAVE HEIGHT, MEAN ENERGY PERIOD, AND THE 4TH MOMENT FOR EACH OF THE HAWAII MODELS, H1 AND H2, USING ST1 AND ST6 PACKAGES AND ALL HAWAII DATA SOURCES FOR THE WINTER PERIOD.....27



## 1 INTRODUCTION

Simulating Waves Nearshore (SWAN, Booij et al. 1996) is one of the two phase-averaged spectral wave models used by the U.S. Navy for forecasting waves. To simulate the evolution of waves, SWAN solves the action density equation with source terms, including but not limited to, wind input and wave dissipation.

Early generations of SWAN and other spectral wave models include nonphysical source term parameterizations, notably the representations of wind input and wave dissipation. Because these two source terms are opposing fluxes, inaccuracies hide in the balance of the terms producing apparently accurate growth curves and estimates of bulk parameters like significant wave height and peak period (Babanin et al. 2010). However, individually, the wind input and wave dissipation terms misrepresent their physical processes and result in less than desirable estimates of spectral modes. We refer to the early SWAN generation as Source Term 1 (ST1) to denote the early source term package.

ST1 (Komen et al. 1984, Komen et al. 1994) uses fixed shape parameterizations, an overall mean wave steepness, and a wind input parameterization obtained for light to moderate winds (Tsagareli et al. 2010, van Vledder et al. 2016). For conditions of mixed wind sea and swell, problems arise. Oftentimes, the model overestimates/underestimates the dissipation of wave energy at low/high frequencies with respect to observations (Ardhuin et al. 2010, van Vledder et al. 2016). Furthermore, “the dissipation term considers all waves breaking all the time with all wave systems affecting the strength of dissipation of all other systems in a physically implausible manner” (Rogers et al. 2003). Model results improve significantly by including more physically based features in the source term parameterizations (Ardhuin et al. 2010).

In slightly more than the last decade, a series of studies provided physically-, observation-based improvements to source term parameterizations, especially in the wind input and dissipation terms. Ardhuin et al. (2010) acknowledge that nonstandard, complex situations benefit most from improved physics and shows that wave growth in the presence of swell and at a slanting fetch to be such situations. Babanin et al. (2010) add extreme wind-wave conditions to the list of benefiting situations. Rogers et al. (2012) selected several improvements for implementation in SWAN. We refer to the new, improved source term package as ST6 and detail the improvements.

Donelan et al. (2005, 2006) develop the wind input parameterization from direct measurements of surface elevation and pressure. The work includes calibration and testing of the parameterization. The improved wind input parameterization incorporates two newly observed features of wind-wave coupling, 1) the dependence of growth on wave steepness and 2) full airflow separation in extreme wind forcing situations (Tsagareli et al. 2010, Rogers et al. 2012). Furthermore, Rogers et al. 2012 adds a physical constraint on the total stress and a drag coefficient based on observational work. Therefore, the wind input parameterization in ST6 equips the model to perform better when simulating well-developed conditions and strongly forced steep, young waves (Donelan et al. 2006, Babanin et al. 2007).

Like the new wind input parameterization, observations led to the ST6 dissipation parameterization (Banner et al. 2000; Babanin and Young 2005; Young and Babanin 2006;

Babanin 2010). The dissipation parameterization improves model performance by physically representing the local and cumulative dissipation as a two-phase function and by implementing a breaking threshold (Rogers et al. 2012). The local dissipation term invokes dissipation for any frequency component where breaking occurs (Ardhuin et al. 2008). Babanin et al. 2010 acknowledges that Donelan 2001 first reports cumulative dissipation resulting from wave breaking caused by compression of short waves riding longer waves. Studies recognize the cumulative dissipation as an important component resulting from the dissipation of smaller waves by turbulence generated by larger, breaking waves (Ardhuin et al. 2010, Babanin et al. 2010, Rogers et al. 2012, and van Vledder et al. 2016). The cumulative dissipation term acts primarily on higher frequencies. In addition to splitting the dissipation into local and cumulative terms, the ST6 package employs a threshold for wave breaking below which no breaking occurs. When the local spectral density falls below a spectral threshold derived from measurements, no breaking occurs at that frequency (Rogers et al. 2012).

Previous studies find a significant improvement in model results with the use of the ST6 parameterizations (van Vledder 2016). As noted previously, the greatest improvements come in models of more complex, specific circumstances, like van Vledder’s study of a strong storm in the Southern North Sea. The improvements come with a price. The improved ST6 parameterizations require additional computational time over the parameterizations included in the ST1 package.

Because operational, computational resources are limited and because model simulations must complete within the operational timeframe, we conduct a cost-benefit analysis for three test cases. In addition, because the additional computational cost for high grid point density models exceed the expected increase in computational cost, we optimize the ST6 parameterizations.

In the following section, we discuss the cost-benefit analysis approach and metrics. In section 3, we discuss each test case, including the cost-benefit results for each case. Finally, we provide a final discussion and recommendation.

## **2 APPROACH**

We take a parallel approach to the cost-benefit analysis for SWAN models using the ST6 package. For the benefit portion of the study, we perform model validations to determine model improvements resulting from use of the ST6 package in place of the ST1 package. We validate models with statistical data-model comparisons using bulk wave parameters determined from wave spectra. We discuss data sources and processing in section 2.1 and the bulk wave parameters and comparison metrics in sections 2.2 and 2.3, respectively.

For the cost portion of the analyses, we consider the wall-clock times to completion for the model validations, and a ratio of the ST6:ST1 times to completion provide a cost metric. Preliminary results suggest a typical increase of approximately 60%. After finding a more than 100% increase in computational cost for a case with a very large number grid points, we use a new optimized ST6 package source code, “ST6f”, to reduce the computational cost.

Model validation is completed for three geographic test cases in this order—the Gulf of Mexico, Southern California, and Hawaii. Test case validations begin with SWAN 40.91ABC—NRL4.3b, which includes the original ST6 package. During the Southern California model validation, we use a version of SWAN that has an optimized/accelerated ST6. We refer to the two ST6 variants as ST6s and ST6f (for “slow” and “fast”). The only noteworthy difference between the two variants are in computation speed. In idealized experiments using square domain of different sizes, and deep water, the ratios for ST6s:ST1 are 1.64 and 1.64, while the ST6f:ST1 ratios are 1.25, 1.26, and 1.26 [[https://alvin.nrlssc.navy.mil/index.php/SWAN\\_timings](https://alvin.nrlssc.navy.mil/index.php/SWAN_timings)].

The Gulf of Mexico test case originates from previous work at the Naval Research Laboratory. The Southern California and Hawaii test cases originate from operational models at the Naval Oceanographic Office. While the cost-benefit analyses focus on the model source term packages, we make additional modifications to the operational model configurations for optimal use of the ST6 package. These modifications are implemented in models using ST1 and ST6 and include changes to the model frequency range and, when feasible, the propagation scheme.

## 2.1 Data Sources and Quality Control

Two data sources provide wave frequency spectra for comparison with modeled wave frequency spectra. We use buoys owned and maintained by the National Data Buoy Center (NDBC) and a number of Datawell buoys operated by The Coastal Data Information Program (CDIP) and The University of Hawaii/Pacific Island Ocean Observing System (UH/PacIOOS; can be found on the CDIP website).

### 2.1.1 NDBC Buoys

During the study dates, the prevalent NDBC buoy hull type is the 3-meter discus buoy (Table 1). Evidence exists that a hull response function correction for 3-m discus buoys reduces high frequency energy such that the buoy measurements cannot be used to validate the model performance in the upper range of the frequency spectrum (Figure 1 and Figure 2). Therefore, we truncate NDBC buoy spectra at 0.300 Hz. The frequency range for model-NDBC wave spectra comparison (Gulf of Mexico and Southern California) is 0.042 – 0.300 Hz.

### 2.1.2 Datawell Buoys

Datawell buoys are specialized wave buoys with a hull diameter of 0.7 or 0.9 m. This type of buoy can be affected by biofouling (Thomson et al. 2015), which must be detected, as it can harm the hydrodynamic response of the buoy at high frequencies, thereby rendering the upper part of the spectrum unsuitable for comparison. In the absence of biofouling, the frequency range for model-Datawell wave spectra comparison (Southern California and Hawaii) is 0.042 – 0.580 Hz. This implies that the Datawell buoy comparisons herein represent a validation of a larger range of frequencies than those using NDBC buoys. In other words, they are *more comprehensive*.

## 2.2 Comparison Parameters

To determine model performance, we calculate bulk parameters (i.e., significant wave height, mean energy period, and the fourth spectral moment) from the models' energy spectra and compare with those calculated from the observed energy spectra. More specifically, the quantities

used for comparison are spectral moments or calculated using spectral moments. A spectral moment is defined by:

$$m_n = \int_0^{\infty} f^n E(f) df.$$

Significant wave height ( $H_{m0}$ ) is related to the total energy of the spectrum,  $m_0$ :

$H_{m0} = 4\sqrt{m_0}$ . This is the most commonly used parameter in wave validation studies.

Mean energy period ( $T_E$ ) is found using the ratio of the spectral moments  $m_{-1}$  and  $m_0$ :

$T_{-1,0} = \frac{m_{-1}}{m_0}$ . This parameter is typically slightly shorter than the peak period  $T_p$ , but closer to  $T_p$

than other commonly used mean period parameters. Since it is calculated via integration, it tends to be more smooth and stable than the peak period, which can only give values corresponding to the discrete frequency bins. The third bulk parameter considered  $m_4$ , is proportional to mean square slope (mss) and is sensitive to the energy at higher frequencies of the spectrum:

$$m_4 = \int_0^{\infty} f^4 E(f) df \text{ (Saulnier et al. 2011).}$$

## 2.3 Comparison Metrics

Before performing any comparisons, the observations and the model output are temporally collocated. For each individual station, time-value pairs exist for each bulk parameter – one calculated from the modeled spectrum and one calculated from the observed spectrum.

### 2.3.1 Time Series Comparisons

We use time series comparisons to provide qualitative analyses of the model validations. For each station, we plot modeled and observed time-value pairs of a station's wave or wind parameters. The time series plots serve 1) to detect any problems with the model configuration, 2) to detect biofouling of Datawell buoys (as the observed values of  $m_4$  will be systematically lower than the modeled values), and 3) to determine if anomalies in statistical comparisons arise from a particular station.

### 2.3.2 Statistical Comparisons

Model performance metrics are based on direct model-data comparison rather than on the comparison of time-value pairs. For each collocated pair of spectra, the bulk parameter value (e.g.,  $H_{m0}$ ) calculated from the model spectrum is plotted against the value of that parameter calculated from the observed spectrum. This technique produces scatter plots, and perfect agreement of the values calculated from each type of spectrum (modeled and observed) would result in all data lying on the diagonal line  $y=x$ . Because the number of model-data pairs is large in many cases, the individual points can overlap in such a way that the density of the points representing model-data pairs cannot be detected; therefore, contour plots are also used to represent the distribution of the points. The points from ST1 vs. observations are plotted alongside those from ST6 vs. observations. This serves to highlight the differences in the performance of the two-source term packages, being that is the only difference between the SWAN ST1 and ST6 simulations.

Performance metrics are calculated to quantify the agreement of each model's results with the observations (ST1 and ST6). The metrics calculated for each comparison are bias, root mean square error (RMSE), the correlation coefficient (CC), normalized bias (NBIAS), and the scatter index (SI).

## 2.4 Model Settings

### 2.4.1 Frequency Range

Determination of the appropriate frequency range is not limited to the observed spectra. Model evaluation involves considering whether all relevant frequencies are included. Guidance to make this decision is based on analysis of observed spectra. Two model frequency lower limits were considered:  $f_{min}=0.0418$  and  $0.0500$  Hz. Energy in the observed spectrum below the model lower limit was calculated for each. For locations where long swell is a component of the wave climate, omitting the energy in the frequency band between the two lower limits tested can lead to an incomplete characterization of model performance and under prediction of significant wave height. For example, in the summer test case shown in Figure 3, taking a sum of the energy in the low frequency bins omitted by using the lower limit of  $0.0418$  Hz (NRL) and dividing it by the total energy yields  $0.10\%$  energy omitted. For the lower limit of  $0.0500$  Hz (NAVO), the result yields  $0.25\%$  omitted. This amounts to NRL missing  $1.20$  cm in wave height (average for each spectrum) and NAVO missing  $1.89$  cm. For winter, the results are: NRL energy missing =  $0.25\%$ , NAVO energy missing =  $0.91\%$ , NRL missing wave height =  $3.11$  cm, NAVO missing wave height =  $5.90$  cm (Figure 4). The effect of this missing energy may seem negligible when considering the average missing wave height for each spectrum, but looking at the plots one can see that the missing energy is concentrated in a few swell events. Under prediction of wave height from the omission of energy could be impactful for those events.

The setting suggested by NRL,  $f_{min}=0.0418$  Hz, is more conservative than the existing  $f_{min}=0.05$  Hz but is not conservative in the absolute sense, as evidenced by the  $0.10\%$  and  $0.25\%$  energy still missing. We also offer a more striking example. Ardhuin et al. (2016) look at two storm events in the North Atlantic which sent swells toward a tiltmeter in the Arctic which measured their passage. They state that both storms generated peak periods above  $25$  s. This implies that a model with  $f_{min}=0.0418$  Hz would not be able to model a majority of the energy in this storm, implying a large underestimation of significant wave height. An  $f_{min}=0.05$  Hz would be much worse. Though beyond the scope of the present study, it may be worthwhile to quantify the missing energy for either selection in context of *extreme events*, e.g. the globally highest wave event of each month for a period of several years.

The NRL  $f_{min}$  matches that which was used—until recently—by the FNMOC-MRY (Fleet Numerical, Monterey) global WAVEWATCH III® (WW3) implementation, rounded from  $0.04177$  Hz. That, in turn, follows an example provided with the version 1 release of NCEP’s WW3, circa 1997. The example given by NCEP in v5 of WW3 is  $0.04118$  Hz. FNMOC-MRY recently changed  $f_{min}$  in their global model to  $0.035$  Hz (P. Wittmann, personal communication).

Significantly, in 1988, the WAM group was using  $f_{min}=0.042$  Hz (WAMDIG 1988) with their  $3^\circ \times 3^\circ$  resolution global model. At that time, computers were obviously less powerful than today, so it is sensible that we should not move to a more limited frequency grid today. We recommend that the default  $f_{min}$  for FNMOC SWAN should be lowered to either  $0.042$  Hz or  $0.035$  Hz (matching WAM of the 1980s or the global FNMOC-MRY model, respectively), with non-default higher selection, e.g.  $f_{min}=0.05$  Hz, in cases where the climatology justifies it. All lakes

and enclosed and semi-enclosed seas probably fall into the latter category, but we have not investigated this.

## **2.4.2 Computational Details**

We run all models on the Cray XC40 “Gordon”. The PGI compiler is used. Simulations use 32 processors on one node of Gordon. We cold-start each model. However, for models requiring more than eight wall clock hours to complete, we split the models into segments and hot-start all segments following the first segment, which uses a cold start.

## **3 TEST CASES**

### **3.1 Gulf of Mexico (GoM)**

The GoM test case was derived from previous Naval Research Laboratory (NRL) work. Because the GoM case is a standard case largely devoid of the complexities of a mixed sea, i.e. the presence of swell, or, in this study, extreme wind input, we expect minimal differences between models using the ST1 and ST6 packages. We note that in extreme wind events, we expect the GoM models using the ST6 package to show significant improvement.

#### **3.1.1 Data Collection**

In the Gulf of Mexico study, area observations are available from buoys owned and maintained by the National Data Buoy Center (NDBC).

#### **3.1.2 Model Setup and Execution**

##### **3.1.2.1 Grids**

The Gulf of Mexico (GoM) test case is a three-grid configuration (Figure 5). We refer to the host, first nest, and second nest as G1, G11, and G112, respectively. See Table 2 for grid properties. Note that each grid contains fewer than 22,000 grid points.

##### **3.1.2.2 Inputs and Settings**

Grids G1 and G11 use bathymetry derived from the Naval Research Laboratory Digital Bathymetry Data Base 2-minute resolution (The Naval Research Laboratory 2017; Marks and Smith 2006). DBDB2 is a global topography data set on a uniform grid developed for ocean modeling. The Coastal Relief Model (CRM) provides bathymetry for the highest resolution grid, G112. The CRM utilizes data from numerous sources to provide a 3-arc second bathymetric and topographic database for the coasts of the continental United States, Hawaii, and Puerto Rico (NOAA 2017).

The COAMPS Central America model provides atmospheric input for the three GoM models, G1, G11, and G112. COAMPS Central America provides information on a 0.2-degree regular grid every three hours. A comparison of wind input to wind data at Buoy 42012 validates the input field (Figure 6).

G1, G11, and G112 employ the second order propagation scheme with wave age set to 12 hours, 6 hours, and 6 hours, respectively.

All models in the GoM test case cover one calendar year dating 2010 July 1 to 2011 June 30 and run in nonstationary mode. G1 and G11 use a 10-minute time step of 10 minutes. G112 requires a reduced time step of 6 minutes.

### 3.1.2.3 Computational Details

The GoM test case uses SWAN run with ST1 and ST6s packages resulting in two instances of each model. The calendar year G1 and G11 models complete in a single submission to the run queue. Because the calendar year G112 models require more than 8 hours to complete, we submit the models to the run queue in a series of 3-month intervals. A sum of the interval's wall clock times to completion in minutes gives the total wall clock time for the G112 models.

G1 and G11 give ST6s:ST1 wall clock time ratios of 1.61. G112 gives a ratio of 1.53. These ratios agree with reports from previous studies<sup>1</sup>.

### 3.1.3 Data-Model Comparison

Data-model comparisons of significant wave heights show little difference in results with respect to the source term package used, regardless of the model (G1, G11, and G112) (Figure 7, Figure 8, Figure 9, left panels). With values of 0.90 or better, correlation coefficients of significant wave height for models G1, G11, and G112 indicate model-data agreement (Table 3). Additional metrics bias, root mean square error, and scatter index show only slight improvements when ST6 is used (Table 4).

Data-model comparisons of mean energy period indicate slight model improvement with the use of the ST6 package (Figure 7, Figure 8, Figure 9, middle panels). The correlation coefficient increases by 0.3 or less with the use of the ST6 package for the GoM models (Table 3). With respect to root mean square error and scatter index, G1, G11, and G112 compare slightly better to data when ST6 is used. With the use of ST6, bias values become more negative, equal, and more positive for G1, G11, and G112, respectively (Table 5).

Data-model comparisons of the 4<sup>th</sup> moment (Figure 7, Figure 8, Figure 9, right panels) show slight improvement with the use of ST6 in the form of slightly elevated correlation coefficients for models G1, G11, and G112 (Table 3). However, with the use of ST6, model-data comparisons show increased normalized bias and no change in scatter index for G1 and G11. Likewise, G112 model-data comparisons result in no change in scatter index but result in a decreased normalized bias in  $m_4$  when ST6 is used (Table 6).

In general, we find that correlations improve, albeit slightly, with the increased grid resolution from G1 to G11. However, we find a decrease in model skill for G112 with respect to the host models. Additional comparisons of G1 and G11 to data from only Buoy 42012 result in significant wave height and 4<sup>th</sup> moment correlation coefficients identical in value to the correlation coefficients for G113 (Table 7). Only the mean energy period parameter shows improvement in model-data correlation with increased model resolution. With the ST1 package the mean energy period correlation increases by 0.4 from G1 to G112; with the ST6 package, it

---

<sup>1</sup> For readers within the navy.mil domain, see [https://alvin.nrlssc.navy.mil/index.php/SWAN\\_timings](https://alvin.nrlssc.navy.mil/index.php/SWAN_timings).

increases by 0.3. The mean energy period and 4<sup>th</sup> moment correlation coefficients improve by 0.2 or less when the ST6 package is used.

### **3.1.4 Discussion**

As expected, models of the GoM benefit little from the use of the ST6s package but result in an approximately 60% increase in computational cost. Predictions of significant wave heights compare well to buoy data with correlations of at least 0.90 regardless of the source term package used in the model or model resolution. The mean energy period and 4<sup>th</sup> moment predictions using ST1 leave room for improvement. Of the two parameters, we find that the mean energy period benefits most from using the ST6 package. Not surprisingly, the 4<sup>th</sup> moment shows the least improvement when the ST6 package is used in place of the ST1 package. We note that in the case of an extreme wind event, the results of this test case would likely change.

## **3.2 Southern California (SoCal)**

The SoCal test case originates from the operational, four-grid model system covering the Southern California coastal area plus a high-resolution model of the Camp Pendleton coast. The operational models horizontally resolve areas to 6 minutes, 2 minutes, 30 seconds, 12 seconds, and 3 seconds.

### **3.2.1 Data Collection**

In the Southern California study area observations are available from both NDBC buoys (Table 8) and Datawell buoys operated primarily by The Coastal Data Information Program (CDIP; see Table 9.). Buoys found in nested models that are not included in hosting models are unresolved in the host model.

### **3.2.2 Model Setup and Execution**

#### **3.2.2.1 Grids**

The SoCal test cases uses a 3-grid system with resolutions of 3 minutes, 12 seconds, and 3 seconds (Figure 10). We refer to the models as Cal1, Cal2, and Cal 3, respectively, and provide model grid parameters in Table 10.

#### **3.2.2.2 Inputs and Settings**

We use the operational bathymetry files for the SoCal models. The files resolve the bathymetric surface to 3 minutes, 12 seconds, and 3 seconds, for the Cal1, Cal2, and Cal3 areas, respectively. The three bathymetric surfaces limit depth to 200 meters. See Figure 11.

Wind input originates from the COAMPS SOCAL model. The model provides wind input on a regular grid resolved to 0.15 degrees in the x- and y-directions at an hourly rate. Figure 12 shows comparisons of the input wind speeds and directions to observations at NDBC Buoy 46047.

A WAVEWATCH III<sup>®</sup> (WW3) (WAVEWATCH III<sup>®</sup> Development Group 2016) implementation provides boundary conditions for Cal1. This WW3 hind cast is from a 1/4° global grid design which uses a regular latitude/longitude grid at low latitudes and irregular polar

stereographic grids at high latitudes. It uses ST4 physics (Ardhuin et al. 2010)<sup>2</sup>. For wind forcing, it used archives of the FNMOC global operational model, and corresponding ice analysis from passive microwave radiometer.

Cal1 uses the second order propagation scheme with a wave age of 2.0 hours. The Cal2 and Cal3 models follow the operational configurations and use the first order “BSBT” propagation scheme. Optimization of propagation settings for Cal2 and Cal3 is beyond the scope of the present work.

The SoCal test case includes two validation periods. We consider the summer period of 2016 July thru 2016 August. The period 2017 January thru 2017 February represents winter conditions.

### 3.2.2.3 Computational Details

The SoCal test case uses a combination of ST1, ST6s, and ST6f.

We use ST1 and ST6s for Cal1 for the summer and winter periods using both source term packages, ST1 and ST6, resulting in four model simulations. All simulations use nonstationary mode with a computational time step of 15 minutes. Considering all four simulations, the cumulative model time to completion ratio ST6s:ST1 is 1.66. The ratio for Cal1 agrees with the ratios for the GoM test case and previous studies.

To evaluate the transition from ST6s to ST6f, both variants provide results for Cal2. All simulations use nonstationary mode with a time step of 15 minutes.

We begin the Cal2 cost-benefit analysis with ST1 and ST6s. Because of the large number of grid points (1, 080, 000) of Cal2, we divide the summer and winter time periods each into nine simulations of 7 days to satisfy the schedule on Gordon. The number of simulations multiply again by two to account for the two source term packages, ST1 and ST6s, resulting in 36 simulations. To determine the ST6s:ST1 time to model completion ratio, we sum the time to completion of models using the ST1 package and sum the time to completion of the models using the ST6s package. We find ST6s:ST1 to be 2.18 for the Cal2 model. We consider a more than 100% increase in computational expense prohibitive in the operational arena and remind reader that the increase in computational cost of the Cal2 (ST6s:ST1 ratio) significantly exceeds the ratio for Cal1, the GoM test case, and previous studies.

Next, we use the final 7-day segment of the summer, Cal2 model to test the new, optimized SWAN-ST6f code. We find the ST6f:ST1 ratio for this 7-day period is 1.24.

The Cal3 model uses ST1 and ST6f. With a total number of grid points much less than Cal2 and a faster variant of ST6, we needed to use only four simulations of Cal3 to complete the cost-benefit analysis—summer and winter using the ST1 package and summer and winter using the ST6f package. As done for previous test cases, we compare the cumulative time to completion using the ST1 package to the cumulative time to completion using the ST6f package and find an ST6f:ST1 ratio of 1.35.

---

<sup>2</sup> We note that ST6 is also available in WW3, but we prefer WW3/ST4, since WW3/ST6 at time of writing is lagging behind the development of WW3/ST4 and SWAN/ST6.

### 3.2.3 Data-Model Comparison

With respect to significant wave height, correlation coefficients of 0.95 and higher during winter and 0.84 during summer show that Cal1 (Figure 13 and Figure 14, left panels) and Cal2 (Figure 15 and Figure 16, left panels) agree with observations. The use of the ST6 package improves the estimates of significant wave height only slightly, mostly during the summer season with improvements in correlations of 0.03 or less (Table 11 and Table 12). Using the ST6 package results in bias, root mean square error, normalized bias, and scatter index that are as good as or better than when using the ST1 package in the Cal1 and Cal2 models (Table 13 and Table 16). Significant wave heights produced by Cal3 show less agreement with the data (Figure 17, right panels), especially during summer when correlations dip to 0.7, and use of the ST6 package decreases correlation coefficients by 0.01 (Table 11 Table 12).

Cal1 (Figure 13 and Figure 14, middle panels) and Cal2 (Figure 15 and Figure 16, middle panels) simulations produce mean energy periods that compare reasonably well to data when using the ST6 package. When ST1 is used, Cal1 and Cal2 compare reasonably well to the NDBC buoys (Table 11). However, when compared to data from the Datawell buoys, the Cal1 and Cal2 models using the ST1 package show a weaker correlation to the data. When compared to the Datawell buoys, Cal1 and Cal2 models using ST6 improve mean energy period correlation coefficients by up to 0.12 (Table 12). Although mean energy periods from the Cal3 models show a general, weaker correlation to data, using ST6 increases the correlation by 0.09 for summer and 0.15 for winter (Table 11 and Table 12).

The largest improvements with the use of the ST6 package appear in the data-model comparisons for the 4<sup>th</sup> moment. With the exception of comparing models using the ST1 package to Datawell buoys, Cal1 (Figure 13 and Figure 14, right panels) and Cal2 (Figure 15 and Figure 16, right panels) model-data comparisons result in correlation coefficients of about 0.8 or higher (Table 11). When compared to Datawell buoys, the ST1, Cal1 and Cal2 model-data comparisons give correlation coefficients less than 0.75. However, we see the largest improvements with the use of the ST6 package in correlation coefficients when we compare Cal1 and Cal2 to Datawell buoys (Table 12) (note: this represents an evaluation of a more complete frequency range than is the case with the NDBC buoys). The correlation coefficients increase by as much as 0.25. Improvements in bias, root mean square error, normalized bias, and scatter index further support the improved correlation coefficients (Table 15 and Table 18). Like the Cal1 and Cal2 models, Cal3 shows significant improvement when ST6 is used (Figure 17, right panel). The Cal3 model is compared to only Datawell buoys, and for the winter period, the correlation coefficient increases by 0.51 when the ST6 package is used. However, we note that overall the correlation coefficients are low for Cal3, 0.76 and 0.51 when the ST6 package is used in the winter and summer, respectively (Table 12).

### 3.2.4 Discussion

Because of the presence of wind sea and swell components in the wave field, the Southern California models are more sensitive to the source term packages. The lower order wave parameter, significant wave height, is the least sensitive to changes in the source term package with changes of 0.3 or less in the correlation coefficients. The mean energy period is sensitive to changes in the source term package when the data-model comparison occurs over a frequency range that includes a larger portion of the spectral tail, i.e. for the Datawell buoys. The high

frequency cut-off of data-model comparisons using the NDBC buoys restricts the cost-benefit analysis. The sensitivity of the data-model comparison to data source is most evident in the analyses of the 4<sup>th</sup> moment for the Cal1 and Cal2 models. For both models, regardless of season or source term package, the model appears to be more accurate when compared to the NDBC buoys because the comparison frequency range is limited. As expected, the data-model comparisons of the 4<sup>th</sup> moment using the Datawell buoys (with their larger frequency range) show the greatest benefit to using the ST6 package in place of the ST1 package for all Southern California models.

We do not make analyses with respect to model resolution because we compare each Southern California model to an independent set of buoys. However, we note a general decrease in accuracy of Cal3 with respect to the Cal2 model, and an increase in the ST6:ST1 time to completion ratio despite the Cal2 model requiring significantly more computations. We suggest a more thorough examination of the model configuration, especially in terms of the choice between STATIONARY or NONSTATIONARY model modes.

We consider the improved predictions of the high frequency wave components by Cal1 and Cal2 to be worth the additional 24% computational cost (ST6f:ST1).

### **3.3 Hawaii**

#### **3.3.1 Data Collection**

In the Hawaii study area, observations are available from Datawell directional buoys (Table 19) operated by The University of Hawaii/Pacific Island Ocean Observing System (UH/PacIOOS; can be found on the CDIP website).

#### **3.3.2 Model Setup and Execution**

##### **3.3.2.1 Grids**

The Hawaii test case is a two-grid system. The host model H1 has a horizontal resolution of 2 minutes, and the nest H2 has a resolution of 12 seconds. See Figure 18. Refer to Table 20 for grid properties.

##### **3.3.2.2 Inputs and Settings**

We use operational bathymetry products for the H1 and H2 models. The bathymetry is horizontally resolved to 30 seconds and 3 seconds, respectively.

Wind input originates from the COAMPS Hawaii\_n3 model. The model provides wind input on a regular grid resolved to 0.05 degrees in the x- and y-directions at an hourly rate.

A WW3 model provides boundary conditions for the test case host model H1. WW3 design is the same as that described in Section 3.2.2.2.

H1 uses the second order propagation scheme with a wave age of 1.0 hours. H2 uses the first order BSBT propagation scheme. Using the second order propagation scheme with H2 requires an increase in model directions to 45, a wave age of 0.25 and a time step of 1.0 minutes. With

these settings, the model's computational cost is prohibitive in the scope of the validation. We recommend considering the Stationary mode for H2, but the consideration is not made in the validation.

### **3.3.2.3 Timeframe**

The Hawaii test case includes two validation periods. We consider the summer period of 2016 July thru 2016 August. The period 2017 January thru 2017 February represents winter conditions.

### **3.3.2.4 Computational Details**

The Hawaii H1 model uses ST1 and ST6f source term packages for the summer and winter periods, for four simulations. The H2 simulation of the summer period using the ST1 package fails to produce results; therefore, we consider only three simulations for the summer period. All simulations use nonstationary mode with a computational time step of 15 minutes. Considering all four simulations, the cumulative model time to completion ratio ST6f:ST1 is approximately 1.5 for the H1 model. Considering only the winter period, the ST6f:ST1 time to completion ratio is 1.37 for the H2 model.

### **3.3.3 Data-Model Comparison**

Like the previous two test cases, we see minimal improvement in significant wave height estimates with the use of the ST6 package (Figure 19 and Figure 20, left panels). Overall, modeled significant wave heights compare well to data sources with correlation coefficients of at least 0.89 (Table 21 and Table 22). For summer and winter, significant wave height predictions from the higher resolution H2-ST6 model are only as good as the predictions from the lower resolution H1-ST1 model. With the given model setups, increasing model resolution and using the improved physics package provides no improvement in results.

Estimates of mean energy period experience no change in agreement with data sources with respect to a change in the source term package used in the model. The previous statement holds for the H1 and H2 models and the summer and winter periods (Table 21 and Table 22).

Like the SoCal test case, estimates of the 4<sup>th</sup> moment benefit most from the improved source term parameterizations of ST6 (Figure 19 and Figure 20, right panels). For the winter period, correlation coefficients improve by 0.2 or more for H1 and H2 (Table 22). Correlation coefficients for the H1 model during the summer period improve by 0.24.

### **3.3.4 Discussion**

With the exception of the comparisons of mean energy period, we find minimal/significant improvements in model estimates of significant wave height/4<sup>th</sup> moment when the Hawaii models employ the ST6 package over the ST1 package. The improvements require an increase of 35-50% in computational expense (ST6f:ST1).

Again, the summer period proves to be the most difficult to model for H1 and, especially, H2. Like the Cal3 simulations, the benefit analysis is limited to the effects of the source term packages. We recommend a more thorough evaluation of the Hawaii test case model configurations.

## 4 CONCLUSIONS

In this work, we conduct a cost-benefit analysis for the SWAN ST6 package. The ST6 package includes enhancements to the wind input and wave dissipation parameterizations. Previous work shows a marked improvement in model accuracy when using the ST6 package, most notably for nonstandard, complex model applications. In the presence of high wind inputs and/or a mixed sea state, higher order wave parameters determined from predicted wave spectra benefit most from using the ST6 package.

Use of the ST6 package requires additional computational resources. In an operational modeling environment users consider computational cost when configuring models to ensure that product deliveries meet operational time constraints.

We evaluate three test cases using the ST1 and ST6 packages to quantify model improvements and to determine the additional computational cost of the use of the ST6 package. The first test case includes three nested models of the Northern Gulf of Mexico and represents a standard model situation with moderate wind input and little to no wave swell. The Gulf of Mexico test case excludes rare, extreme weather events like hurricanes. The other two test cases included nested models of Southern California and Hawaii. These models represent complex model situations with moderate wind input conditions but a mixed wave state.

The Gulf of Mexico test case shows little improvement in significant wave height, mean energy period, and 4<sup>th</sup> moment wave parameters when models use the non-optimized ST6s package but requires 60% more computational time than when models use the ST1 package. The Gulf of Mexico models show that the ST6 package is not useful for models with moderate wind input and/or an absence of swell.

Both the Southern California and Hawaii test case models contain moderate wind input but mixed wave fields. In these test cases, the models using the ST6 package see moderate improvements in low order wave parameters, significant wave height and mean energy period. We find the most pronounced model improvements in the 4<sup>th</sup> moment wave parameter. We reduce early, prohibitive increases in computational costs, most notable for the Cal2 model, to 50% or less by optimizing the ST6 package (ST6f). For all cases which used optimized ST6f within this report, the computation time ratios (ST6f:ST1) are: 1.24:1, 1.35:1, 1.49:1, and 1.37:1.

The cost-benefit analysis applies to the SWAN source term packages, ST1 and ST6. However, the authors recommend the evaluation of other model settings, especially for the higher resolution, Cal3 and H2, models.

## 5 RECOMMENDATIONS

### *SWAN operation*

- 1) *Source term package*: ST6 should be used in regions exposed to swells generated in the Atlantic, Pacific, Indian and Southern Oceans. In enclosed and semi-enclosed seas, e.g.

Gulf of Mexico, North Sea, Mediterranean Sea, Adriatic Sea, ST1 can be used, unless or until subsequent studies in those areas indicate a significant skill penalty when using ST1.

- 2) *Frequency grid*: We recommend that the default starting frequency of the FNMOC SWAN implementations be reduced from the present  $f_{min}=0.05$  Hz. Two possibilities are suggested: a) (less conservative) match that used for WAM in the 1980s,  $f_{min}=0.042$  Hz, or b) (more conservative) match that of the FNMOC-MRY global WW3 model, presently  $f_{min}=0.035$  Hz. However, 0.05 Hz can be retained as a non-default selection where climatology supports this. In enclosed and semi-enclosed seas, the fraction of wave energy below 0.05 Hz is typically small, even in cases of tropical cyclones. Therefore, the higher  $f_{min}$  may be justified. However, such a determination has not been made herein.

#### *Further work*

- 1) The present study did not include comparison of ST1 vs. ST6 in an enclosed or semi-enclosed basin using data from a buoy which can make reliable measurements of higher frequencies (greater than 0.3 Hz). We recommend that this be done.
- 2) Further evaluation of higher resolution nests for computational efficiency, with special attention to computation mode: stationary vs. non-stationary. Also, evaluate time step size, and HPC usage (scaling efficiency).
- 3) Replace large, inefficient SWAN models with WAVEWATCH III (WW3) grids. In particular, using WW3 “coastal grids”, where the grid cells which are in deep water and far from the coast are excluded from computations with a mask, such as the Australia grid demo’d in 2014 [[https://alvin.nrlssc.navy.mil/index.php/WW3\\_timeline](https://alvin.nrlssc.navy.mil/index.php/WW3_timeline)]. See also the Alaska grid in Tolman (2008). Develop metric for identifying the most wasteful SWAN grids; these grids would be given highest priority for replacement.
- 4) Thorough, global evaluation of impact of the user’s choice of minimum computational frequency  $f_{min}$  in terms of % energy omitted on average, and % energy omitted for most severe storm of each month globally, for a period of several years.

## **6 ACKNOWLEDGMENTS**

Datawell buoy data furnished by the Coastal Data Information Program (CDIP), Integrative Oceanography Division, operated by the Scripps Institution of Oceanography, under the sponsorship of the U.S. Army Corps of Engineers and the California Department of Parks and Recreation. Original Southern California and Hawaii model configurations provided by the Naval Oceanographic Office with assistance and from Kelly Wood and Peter Gay. Richard Bouchard, Physical Scientist, NOAA’s National Data Buoy Center, for supplying information about the NDBC buoys’ hull types during the study period.

ST6 optimization method was provided by Marcel Zijlema, TU Delft.

## **7 REFERENCES**

- Ardhuin, F., F. Collard, B. Chapron, P. Queffelec, J-F. Filipot, M. Hamon, 2008: Spectral wave dissipation based on observations: A global validation. Proc. Chinese-German Joint Symp. On Hydraulics and Ocean Engineering, Darmstadt, Germany, Universitat Darmstadt, 391-400.
- Ardhuin, F., W. E. Rogers, A. V. Babanin, J-F Filipot, R. Magne, A. Roland, A. J. Van der Westhuysen, P. Queffelec, J. M. Lefevre, L. Aouf, F. Collard, 2010: Semi-empirical

- dissipation source functions for ocean waves. Part I: definition, calibration, and validation. *J. Phys. Oceanogr.*, 40, 1917-1941.
- Ardhuin, F., P. Sutherland, M. Doble, and P. Wadhams (2016), Ocean waves across the Arctic: Attenuation due to dissipation dominates over scattering for periods longer than 19 s, *Geophys. Res. Lett.*, 43, 5775–5783, doi:10.1002/2016GL068204.
- Babanin, A. V., and I. R. Young, 2005: Two-phase behavior of the spectral dissipation of wind waves. *Proc. Ocean Waves Measurements and Analysis, Fifth Intern. Symp. WAVES2005*, Madrid, Spain, CEDEX, Paper 51.
- Babanin, A. V., K. N. Tsagareli, I. R. Young, and D. J. Walker, 2010: Numerical investigation of spectral evolution of wind waves. Part II: Dissipation function and evolution tests. *J. Phys. Oceanogr.*, 40, 667-683.
- Banner, M. L., A. V. Babanin, and I. R. Young, 2000: Breaking probability for dominant waves on the sea surface. *J. Phys. Oceanogr.*, 30, 3145-3160.
- Booij, N., L. H. Holthuijsen, and R. C. Ris, 1996: The SWAN wave model for shallow water. *Proc. 25th Int. Conf. in Coastal Eng., ASCE, Orlando, FL, ASCE*, 668-676.
- Donelan, M. A., 2001: A nonlinear dissipation function due to wave breaking. *Proc. Workshop on Ocean Wave Forecasting, Reading, United Kingdom, ECMWF*, 87-94.
- Donelan, M. A., A. V. Babanin, I. R. Young, M. L. Banner, C. McCormick, 2005: Wave follower field measurements of the wind-input spectral function. Part I: measurements and calibrations. *J. Atmos. Ocean Technol.*, 22, 799-813.
- Donelan, M. A., A. V. Babanin, I. R. Young, M. L. Banner, 2006: Wave-follower field measurements of the wind-input spectral function. Part II: parameterization of the wind input. *J. Phys. Oceanogr.*, 36, 1672-1688.
- Komen, G. J., S. Hasselmann, and K. Hasselmann, 1984: On the existence of a fully developed wind-sea spectrum. *J. Phys. Oceanogr.*, 14, 1271-1285.
- Komen, G. J., L. Cavaleri, M. Donelan, K. Hasselmann, S. Hasselmann, and P. A. E. M. Janssen, 1994: *Dynamics and Modelling of Ocean Waves*. Cambridge University Press, 532 pp.
- Marks, K. M. and W. H. F. Smith, 2006: An evaluation of publicly available global bathymetry grids, *Marine Geo. Res.*, 27, 19-34.
- Naval Research Laboratory, NRL DBDB2, September 22, 2017, [https://www7320.nrlssc.navy.mil/DBDB2\\_WWW/NRLCOM\\_dbdb2.html](https://www7320.nrlssc.navy.mil/DBDB2_WWW/NRLCOM_dbdb2.html).
- NOAA National Centers for Environmental Information, U.S. Coastal Relief Model, September 22, 2017, <http://www.ngdc.noaa.gov/mgg/coastal/crm.html>.
- Rogers, W. E., P. A. Hwang, and D. W. Wang, 2003: Investigation of wave growth and decay in the SWAN model: Three regional-scale applications. *J. Phys. Oceanogr.*, 33, 366-389.
- Rogers, W. E., A. V. Babanin, D. W. Wang, 2012: Observation-consistent input and whitecapping-dissipation in a model for wind-generated surface waves: description and simple calculations. *J. Atmos. Ocean Technol.*, 29, 1329-1346.
- Saulnier, J. B., A. Clement, A. F. de O. Flacao, T. Pontes, M. Prevosto, P. Ricci, 2011: Wave groupiness and spectral bandwidth as relevant parameters for the performance assessment of wave energy converters, *Ocean Engin.*, 38, 130-147.
- Thompson, J., J. Talber, S. de Klerk, A. Brown, M. Schwendeman, J. Goldsmith, C. Meinig, 2015: Biofouling effects on the response of a wave measurement buoy in deep water. *Journal of Atmospheric and Oceanic Technology*, 32(6), 1281-1286.
- Tolman, H.L. 2008: A mosaic approach to wind wave modeling. *Ocean Modelling*, 25, 35-47.

- Tsagareli, K. N., A. V. Babanin, D. J. Walker, and I. R. Young, 2010: Numerical investigation of spectral evolution of wind waves. Part I: Wind input source function. *J. Phys. Oceanogr.*, 40, 656-666.
- Van Vledder, G. Ph., S. Th. C. Hulst, J. D. McConochie, 2016: Source term balance in a severe storm in the Southern North Sea. *Ocean Dynamics*, 66, 1681-1697.
- WAMDIG (1988). The WAM model – a third generation ocean wave prediction model. *J. Phys. Oceanogr.*, 18, 1775-1810.
- WAVEWATCH III® Development Group, 2016: User manual and system documentation of WAVEWATCH III® version 5.16. Tech. Note 329, NOAA/NWS/NCEP/MMAB, College Park, MD, USA, 326 pp. + Appendices.
- Young, I. R., and A. V. Babanin, 2006: Spectral distribution of energy dissipation of wind-generated waves due to dominant wave breaking. *J. Phys. Oceanogr.*, 36, 376-394.

## 8 TABLES

**Table 1. NDBC Buoy Information for the Gulf of Mexico Test Case.**

STATION ID	HULL TYPE	CAL1	CAL2	CAL3	OPERATOR
42012	3-meter discus	X	X	X	NDBC
42036	3-meter discus to 12/2010 3-meter foam to present	X	X		NDBC
42039	3-meter foam	X	X		NDBC
42040	10-meter steel hull	X	X		NDBC

**Table 2. Grid properties for Gulf of Mexico Test Case, including the number of grid points and lengths in x- and y-directions, the horizontal resolution, and the number of model frequencies and directions.**

MODEL	G1	G11	G112
GRID POINTS, X	100	165	240
GRID POINTS, Y	65	60	90
GRID LENGTH, X	20 degrees	11 degrees	4 degrees
GRID LENGTH, Y	13 degrees	4 degrees	1.5 degrees
RESOLUTION	0.2 degrees	0.067 degrees	0.0167 degrees
FREQUENCIES	33	33	33
DIRECTIONS	36	36	36

**Table 3. Correlation coefficients for comparisons of significant wave height, mean energy period, and the 4th moment for each of the Gulf of Mexico models, G1, G11, and G112, using ST1 and ST6 packages and all Gulf of Mexico data sources.**

MODEL	G1		G11		G112	
	ST1	ST6	ST1	ST6	ST1	ST6
<b>ST PACKAGE</b>						
<b>SIGNIFICANT WAVEHEIGHT</b>	0.91	0.91	0.91	0.91	0.90	0.90
<b>MEAN ENERGY PERIOD</b>	0.65	0.68	0.66	0.69	0.66	0.67
<b>4<sup>TH</sup> MOMENT</b>	0.86	0.87	0.85	0.87	0.85	0.86

**Table 4. Significant wave height performance metrics. Bias, root mean square error (RMSE), normalized bias (NBIAS), and scatter index (SI) for model-data comparisons of Gulf of Mexico Models, G1, G11, and G112.**

MODEL	G1		G11		G112	
	ST1	ST6	ST1	ST6	ST1	ST6
<b>ST PACKAGE</b>						
<b>BIAS</b>	0.08	0.07	0.08	0.07	0.09	0.07
<b>RMSE</b>	0.27	0.25	0.27	0.25	0.24	0.23
<b>NBIAS</b>	0.09	0.08	0.09	0.08	0.11	0.09
<b>SI</b>	0.31	0.29	0.31	0.29	0.30	0.30

**Table 5. Mean energy period performance metrics. Bias, root mean square error (RMSE), normalized bias (NBIAS), and scatter index (SI) for model-data comparisons of Gulf of Mexico Models, G1, G11, and G112.**

MODEL	G1		G11		G112	
	ST1	ST6	ST1	ST6	ST1	ST6
<b>ST PACKAGE</b>						
<b>BIAS</b>	-0.01	0.02	-0.02	-0.02	-0.02	0.04
<b>RMSE</b>	0.76	0.69	0.75	0.68	0.78	0.75
<b>NBIAS</b>	0.00	0.00	0.00	0.00	0.00	0.01
<b>SI</b>	0.16	0.14	0.15	0.14	0.16	0.15

**Table 6. Fourth spectral moment performance metrics. Bias, root mean square error (RMSE), normalized bias (NBIAS), and scatter index (SI) for model-data comparisons of Gulf of Mexico Models, G1, G11, and G112.**

MODEL	G1		G11		G112	
	ST1	ST6	ST1	ST6	ST1	ST6
BIAS	170E-7	230E-7	210E-7	260E-7	250E-7	190E-7
RMSE	830E-7	850E-7	850E-7	870E-7	810E-7	800E-7
NBIAS	0.10	0.13	0.12	0.15	0.16	0.12
SI	0.47	0.47	0.48	0.48	0.50	0.50

**Table 7. Correlation coefficients for comparisons of significant wave height, mean energy period, and the 4th moment for each of the Gulf of Mexico models, G1, G11, and G112, using ST1 and ST6 packages and Buoy 42012.**

MODEL	G1		G11		G112	
	ST1	ST6	ST1	ST6	ST1	ST6
SIGNIFICANT WAVEHEIGHT	0.90	0.90	0.90	0.90	0.90	0.90
MEAN ENERGY PERIOD	0.62	0.64	0.65	0.66	0.66	0.67
4 <sup>TH</sup> MOMENT	0.85	0.86	0.85	0.86	0.85	0.86

**Table 8. NDBC Buoy Information for the Southern California Test Case.**

STATION ID	HULL TYPE	CAL1	CAL2	CAL3	OPERATOR
46011	3-meter discus	X			NDBC
46012	3-meter discus	X			NDBC
46013	3-meter discus	X			NDBC
46014	2.3-meter foam	X			NDBC
46015	3-meter discus	X			NDBC
46022	3-meter discus	X			NDBC
46025	3-meter discus	X	X		NDBC
46027	3-meter discus	X			NDBC
46028	3-meter discus	X			NDBC
46042	3-meter discus	X			NDBC
46047	3-meter discus	X	X		NDBC
46053	2.3-meter foam	X	X		NDBC
46054	3-meter discus	X	X		NDBC

46069	3-meter discus	X	X		NDBC
-------	----------------	---	---	--	------

**Table 9. Datawell Buoy Information for the Southern California Test Case.**

STATION ID	HULL TYPE	CAL1	CAL2	CAL3	OPERATOR
028	Datawell (Mark 3)	X	X		CDIP
029	Datawell (Mark 3)	X			CDIP
043	Datawell (Mark 3)		X	X	USMC
045	Datawell (Mark 3)			X	CDIP
067	Datawell (Mark 3)	X	X		NAVY
071	Datawell (Mark 3)	X	X		CDIP
076	Datawell (Mark 3)		X		CDIP
092	Datawell (Mark 3)	X	X		CDIP
094	Datawell (Mark 3)	X			CDIP
100	Datawell (Mark 3)	X	X		CDIP
111	Datawell (Mark 3)	X	X		CDIP
142	Datawell (Mark 4)	X			CDIP
157	Datawell (Mark 3)	X			CDIP
185	Datawell (Mark 3)	X			NDBC
191	Datawell (Mark 3)	X			CDIP
201	Datawell (Mark 3)		X		CDIP
203	Datawell (Mark 3)	X			NAVY
213	Datawell (Mark 3)	X	X		CDIP
215	Datawell (Mark 3)	X	X		CDIP
216	Datawell (Mark 3)	X	X		CDIP
220	Datawell (Mark 3)	X	X		CDIP
222	Datawell (Mark 3)	X			CDIP

**Table 10. Grid properties for Southern California Test Case, including the number of grid points and lengths in x- and y-directions, the horizontal resolution, and the number of model frequencies and directions.**

MODEL	CAL1	CAL2	CAL3
GRID POINTS, X	280	1200	540
GRID POINTS, Y	268	900	540
GRID LENGTH, X	14 degrees	4 degrees	0.45 degrees
GRID LENGTH, Y	13.4 degrees	3 degrees	0.45 degrees
RESOLUTION	0.05 degrees	0.0033 degrees	0.000833 degrees
FREQUENCIES	33	33	33

<b>DIRECTIONS</b>	36	36	36
-------------------	----	----	----

**Table 11. Correlation coefficients for comparisons of significant wave height, mean energy period, and the 4th moment for each of the Southern California models, Cal1 and Cal2, using ST1 and ST6 packages and NDBC Buoys.**

<b>MODEL</b>		<b>CAL1</b>		<b>CAL2</b>	
<b>ST PACKAGE</b>		<b>ST1</b>	<b>ST6</b>	<b>ST1</b>	<b>ST6</b>
<b>SIGNIFICANT WAVEHEIGHT</b>	WINTER	0.95	0.95	0.95	0.96
	SUMMER	0.84	0.87	0.88	0.89
<b>MEAN ENERGY PERIOD</b>	WINTER	0.86	0.87	0.77	0.81
	SUMMER	0.81	0.81	0.82	0.84
<b>4<sup>TH</sup> MOMENT</b>	WINTER	0.82	0.91	0.81	0.91
	SUMMER	0.79	0.86	0.83	0.87

**Table 12. Correlation coefficients for comparisons of significant wave height, mean energy period, and the 4th moment for each of the Southern California models, Cal1, Cal2, and Cal3 using ST1 and ST6 packages and Datawell Buoys.**

<b>MODEL</b>		<b>CAL1</b>		<b>CAL2</b>		<b>CAL3</b>	
<b>ST PACKAGE</b>		<b>ST1</b>	<b>ST6</b>	<b>ST1</b>	<b>ST6</b>	<b>ST1</b>	<b>ST6</b>
<b>SIGNIFICANT WAVEHEIGHT</b>	WINTER	0.96	0.96	0.96	0.96	0.93	0.92
	SUMMER	0.89	0.92	0.90	0.91	0.71	0.70
<b>MEAN ENERGY PERIOD</b>	WINTER	0.74	0.81	0.62	0.74	0.53	0.68
	SUMMER	0.68	0.75	0.72	0.76	0.63	0.72
<b>4<sup>TH</sup> MOMENT</b>	WINTER	0.61	0.86	0.64	0.86	0.18	0.76

SUMMER	0.62	0.82	0.73	0.85	0.34	0.51
--------	------	------	------	------	------	------

**Table 13. Bias, root mean square error (RMSE), normalized bias (NBIAS), and scatter index (SI) for significant wave height model-data comparisons of Southern California models and NDBC data.**

MODEL		CAL1		CAL2	
		ST1	ST6	ST1	ST6
BIAS	WINTER	0.23	0.09	0.24	0.05
	SUMMER	0.45	0.28	0.41	0.21
RMSE	WINTER	0.46	0.41	0.42	0.34
	SUMMER	0.56	0.41	0.50	0.34
NBIAS	WINTER	0.09	0.03	0.12	0.03
	SUMMER	0.27	0.17	0.29	0.15
SI	WINTER	0.16	0.16	0.17	0.16
	SUMMER	0.20	0.18	0.21	0.19

**Table 14. Bias, root mean square error (RMSE), normalized bias (NBIAS), and scatter index (SI) for model-data comparisons of mean energy period for Southern California models and NDBC data.**

MODEL		CAL1		CAL2	
		ST1	ST6	ST1	ST6
BIAS	WINTER	0.38	0.69	0.10	0.66
	SUMMER	0.85	0.98	0.67	1.06
RMSE	WINTER	1.09	1.19	1.25	1.3
	SUMMER	1.16	1.27	1.15	1.40
NBIAS	WINTER	0.04	0.07	0.01	0.06
	SUMMER	0.10	0.81	0.08	0.13
SI	WINTER	0.10	0.09	0.12	0.11
	SUMMER	0.10	0.12	0.11	0.11

**Table 15. Bias, root mean square error (RMSE), normalized bias (NBIAS), and scatter index (SI) for 4th moment model-data comparisons of Southern California models and NDBC data.**

MODEL		CAL1		CAL2	
		ST1	ST6	ST1	ST6
<b>BIAS</b>	WINTER	130E-7	-560E-7	260E-7	-94E-7
	SUMMER	480E-7	230E-7	510E-7	65E-7
<b>RMSE</b>	WINTER	930E-7	700E-7	820E-7	520E-7
	SUMMER	870E-7	620E-7	760E-7	450E-7
<b>NBIAS</b>	WINTER	0.07	-0.03	0.21	-0.08
	SUMMER	0.35	0.17	0.42	0.05
<b>SI</b>	WINTER	0.52	0.39	0.64	0.42
	SUMMER	0.53	0.42	0.46	0.36

**Table 16. Bias, root mean square error (RMSE), normalized bias (NBIAS), and scatter index (SI) for significant wave height model-data comparisons of Southern California models and Datawell data.**

MODEL		CAL1		CAL2		CAL3	
		ST1	ST6	ST1	ST6	ST1	ST6
BIAS	WINTER	0.21	0.03	0.19	0.01	0.26	0.11
	SUMMER	0.42	0.23	0.39	0.20	0.52	0.35
RMSE	WINTER	0.41	0.34	0.35	0.28	0.35	0.27
	SUMMER	0.49	0.32	0.45	0.29	0.54	0.37
NBIAS	WINTER	0.10	0.02	0.12	0.00	0.25	0.10
	SUMMER	0.31	0.17	0.34	0.17	0.60	0.40
SI	WINTER	0.17	0.16	0.19	0.18	0.22	0.23
	SUMMER	0.19	0.17	0.20	0.19	0.15	0.14

**Table 17. Bias, root mean square error (RMSE), normalized bias (NBIAS), and scatter index (SI) for total energy model-data comparisons of Southern California models and Datawell data.**

MODEL		CAL1		CAL2		CAL3	
		ST1	ST6	ST1	ST6	ST1	ST6
<b>BIAS</b>	WINTER	0.11	0.76	-0.15	0.79	0.10	1.34
	SUMMER	0.68	1.23	0.59	1.42	0.89	2.17
<b>RMSE</b>	WINTER	1.39	1.41	1.66	1.61	1.68	2.03
	SUMMER	1.40	1.66	1.44	1.93	1.57	2.46
<b>NBIAS</b>	WINTER	0.01	0.08	-0.02	0.08	0.01	0.14
	SUMMER	0.08	0.14	0.07	0.17	0.09	0.22
<b>SI</b>	WINTER	0.14	0.12	0.17	0.14	0.18	0.16
	SUMMER	0.14	0.13	0.15	0.15	0.13	0.12

**Table 18. Bias, root mean square error (RMSE), normalized bias (NBIAS), and scatter index (SI) for 4th moment model-data comparisons of Southern California models and Datawell data.**

MODEL		CAL1		CAL2		CAL3	
		ST1	ST6	ST1	ST6	ST1	ST6
BIAS	WINTER	550E-7	-380E-7	720E-7	-430E-7	470E-7	-650E-7
	SUMMER	1700E-7	320E-7	1600E-7	-78E-7	1800E-7	54E-7
RMSE	WINTER	3000E-7	1600E-7	2500E-7	1400E-7	2300E-7	1600E-7
	SUMMER	2900E-7	1400E-7	2400E-7	1100E-7	2300E-7	700E-7
NBIAS	WINTER	0.14	-0.10	0.25	-0.17	0.23	-0.31
	SUMMER	0.58	0.11	0.61	0.00	1.33	0.04
SI	WINTER	0.78	0.41	0.86	0.47	1.08	0.71
	SUMMER	0.76	0.44	0.67	0.41	0.96	0.51

**Table 19. Datawell Buoy Information for the Hawaii Test Case.**

STATION ID	HULL TYPE	H1	H2	OPERATOR
098	Datawell (Mark 3)	X	X	UH/PACIOOS
106	Datawell (Mark 3)	X	X	UH/PACIOOS
165	Datawell (Mark 3)		X	UH/PACIOOS
187	Datawell (Mark 3)	X		UH/PACIOOS
225	Datawell (Mark 3)	X	X	UH/PACIOOS

**Table 20. Grid properties for Hawaii Test Case, including the number of grid points and lengths in x- and y-directions, the horizontal resolution, and the number of model frequencies and directions.**

<b>MODEL</b>	<b>H1</b>	<b>H2</b>
<b>GRID POINTS, X</b>	180	425
<b>GRID POINTS, Y</b>	135	525
<b>GRID LENGTH, X</b>	6 degrees	1.42 degrees
<b>GRID LENGTH, Y</b>	4.5 degrees	1.75 degrees
<b>RESOLUTION</b>	0.03 degrees	0.0033
<b>FREQUENCIES</b>	33	33
<b>DIRECTIONS</b>	36	36

**Table 21. Correlation coefficients for comparisons of significant wave height, mean energy period, and the 4th moment for each of the Hawaii models, H1 and H2, using ST1 and ST6 packages and all Hawaii data sources for the summer period.**

<b>MODEL</b>	<b>H1</b>		<b>H2</b>	
	<b>ST1</b>	<b>ST6</b>	<b>ST1</b>	<b>ST6</b>
<b>SIGNIFICANT WAVEHEIGHT</b>	0.89	0.91	--	0.89
<b>MEAN ENERGY PERIOD</b>	0.86	0.86	--	0.86
<b>4<sup>TH</sup> MOMENT</b>	0.51	0.75	--	0.69

**Table 22. Correlation coefficients for comparisons of significant wave height, mean energy period, and the 4th moment for each of the Hawaii models, H1 and H2, using ST1 and ST6 packages and all Hawaii data sources for the winter period.**

<b>MODEL</b>	<b>H1</b>		<b>H2</b>	
	<b>ST1</b>	<b>ST6</b>	<b>ST1</b>	<b>ST6</b>
<b>SIGNIFICANT WAVEHEIGHT</b>	0.92	0.93	0.91	0.92
<b>MEAN ENERGY PERIOD</b>	0.83	0.83	0.84	0.84
<b>4<sup>TH</sup> MOMENT</b>	0.67	0.88	0.68	0.88

## 9 FIGURES

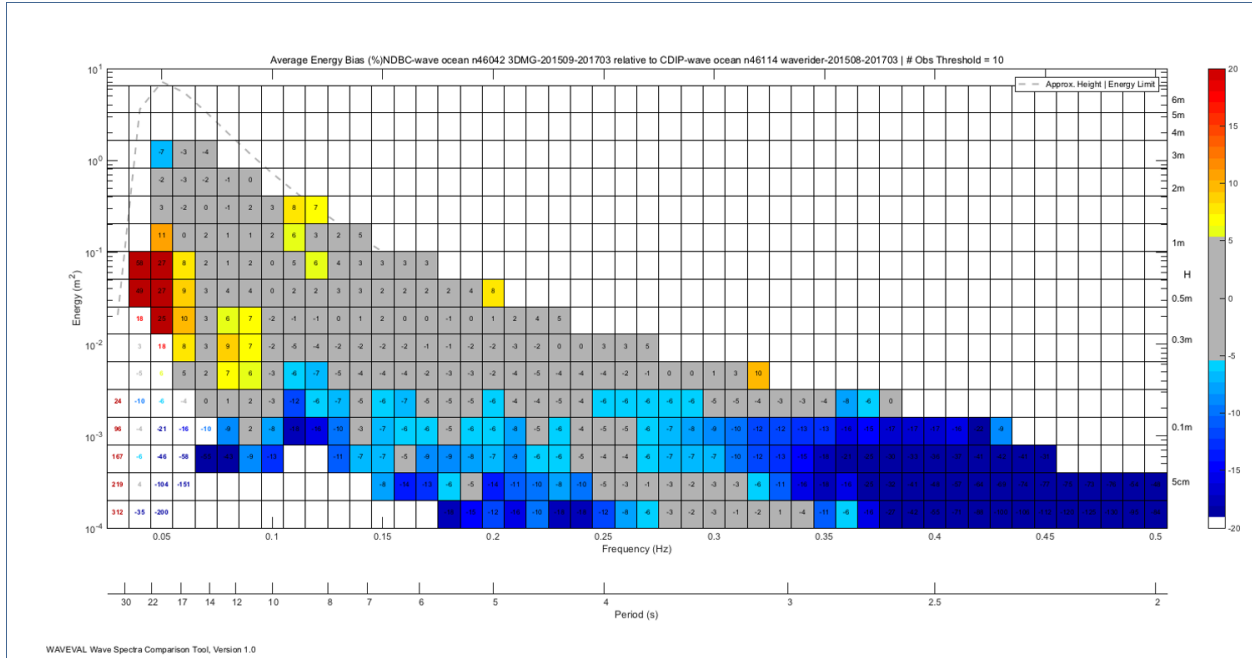


**Figure 1. Provided by Bob Jensen, U.S. Army Corps of Engineers. It indicates that the 3-m discus buoy near Monterey, CA (Station ID 46042) has negative bias (dark blue color) in higher frequencies (right side of plot) compared with a nearby Waverider buoy (Station ID 46114).**

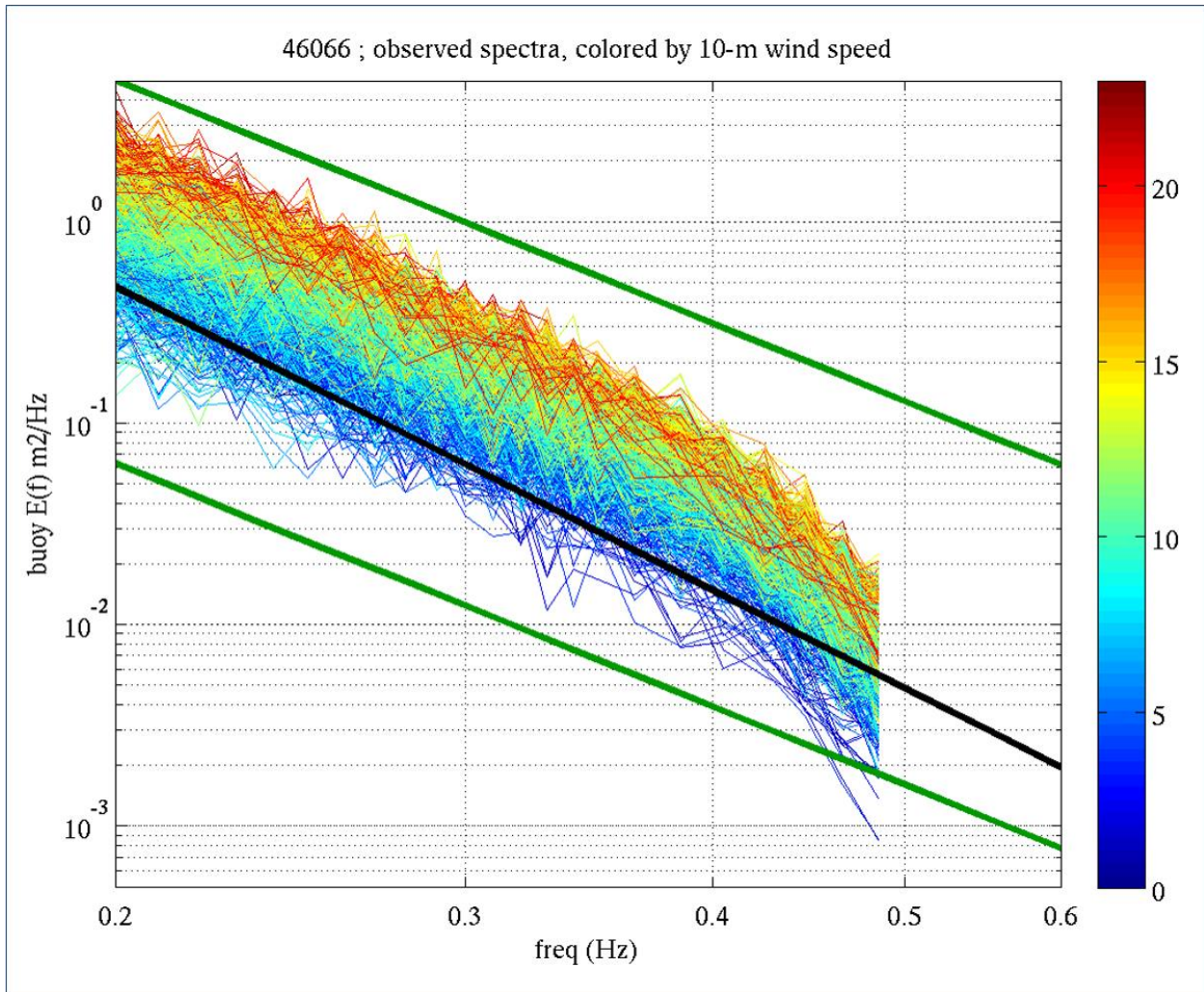


**Figure 2.** A log-log plot of observed spectra from the 3-m discus buoy 310 NM SSW of Kodiak, AK (Station ID 46066), colored by 10 m wind speed. Notice the slope of the spectral tail slope is rather suspect in the 0.3 to 0.485 Hz range, deviating from the expected  $S(f) \propto f^{-4}$  functional form – steepening to approach or exceed  $S(f) \propto f^{-5}$ , indicating that the published spectra are missing energy in the higher frequencies ( $> 0.3$  Hz).

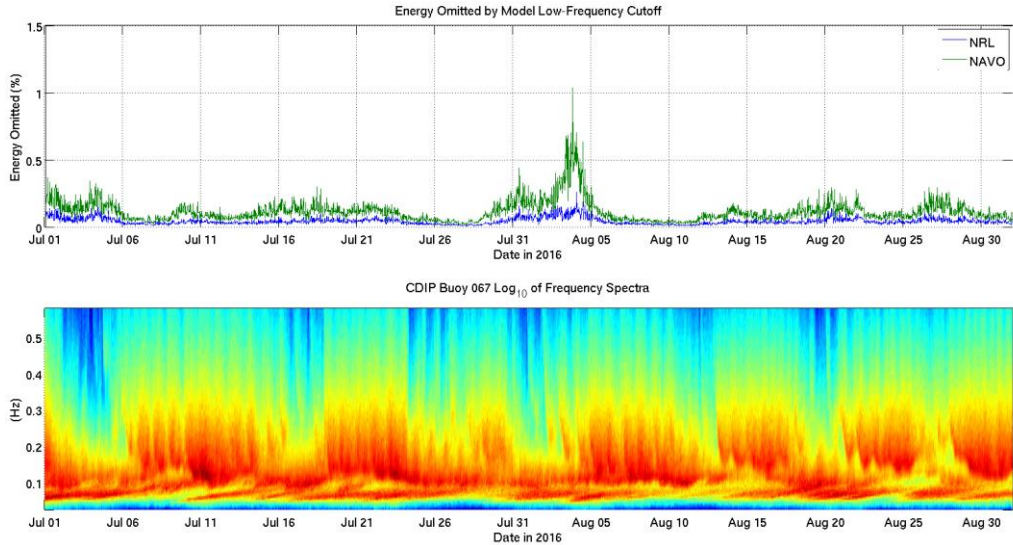


**Figure 3. (top)** The shows the energy omitted for the period of July-August 2016, by NAVO's model lower frequency limit of 0.05 Hz (green curve) and by NRL's model lower frequency limit of 0.0418 Hz (blue curve); **(bottom)** shows the wave frequency spectra for the July-August 2016 Southern California study.

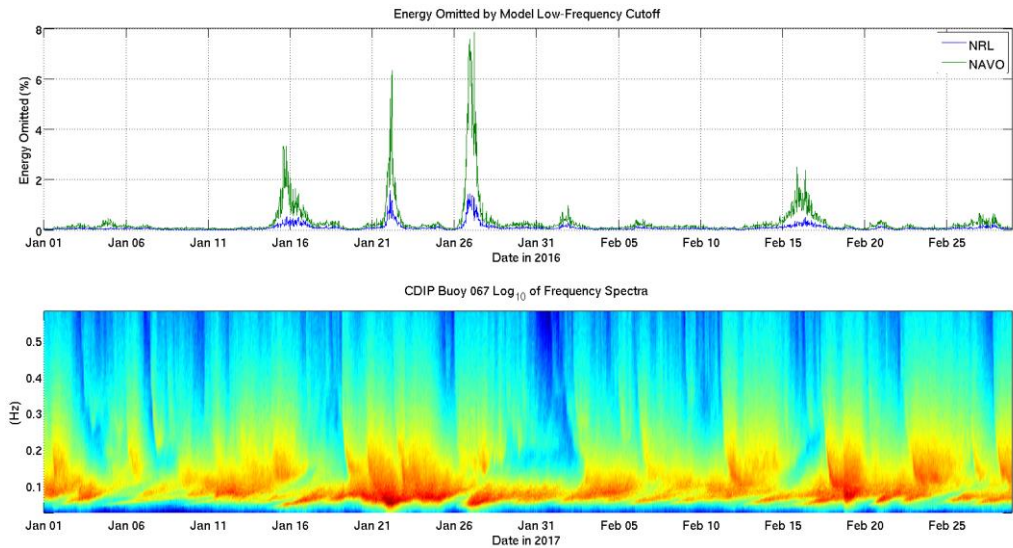


**Figure 4. (top)** The shows the energy omitted for the period of January-February 2017, by NAVO's model lower frequency limit of 0.05 Hz (green curve) and by NRL's model lower frequency limit of 0.0418 Hz (blue curve); **(bottom)** shows the wave frequency spectra for the January-February 2017 Southern California study. The swell events during which the largest quantities of missing energy occur are clearly visible.

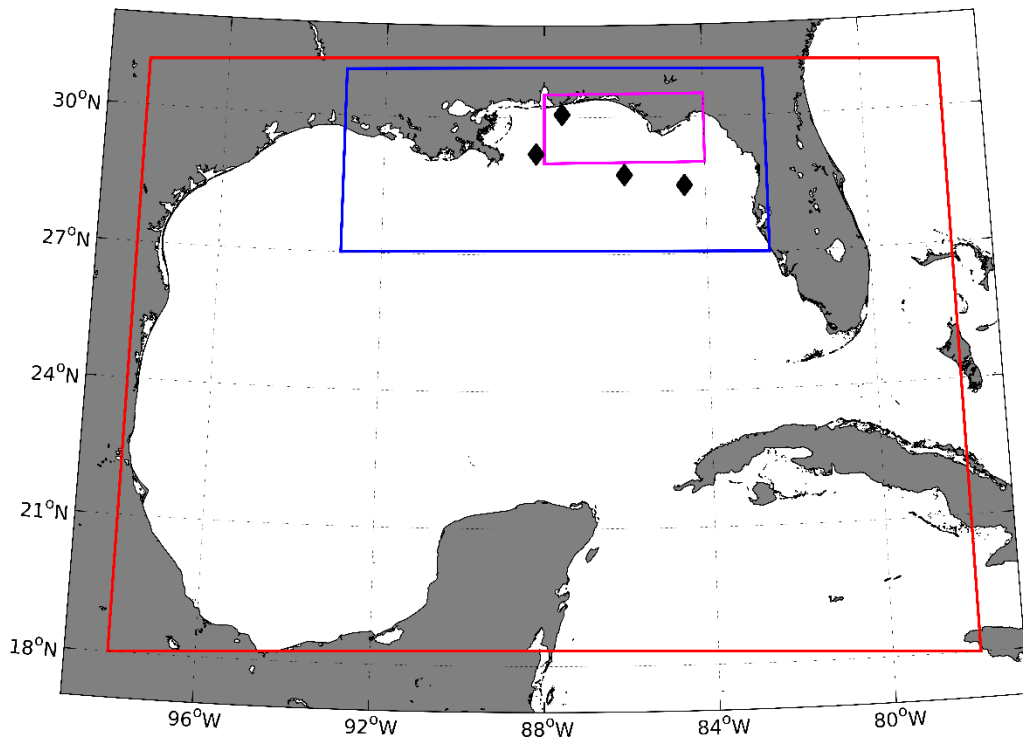


**Figure 5. Model grid configuration for the Gulf of Mexico test case, G1 (red), G11 (blue), G112 (magenta) and NDBC buoys (black diamonds).**

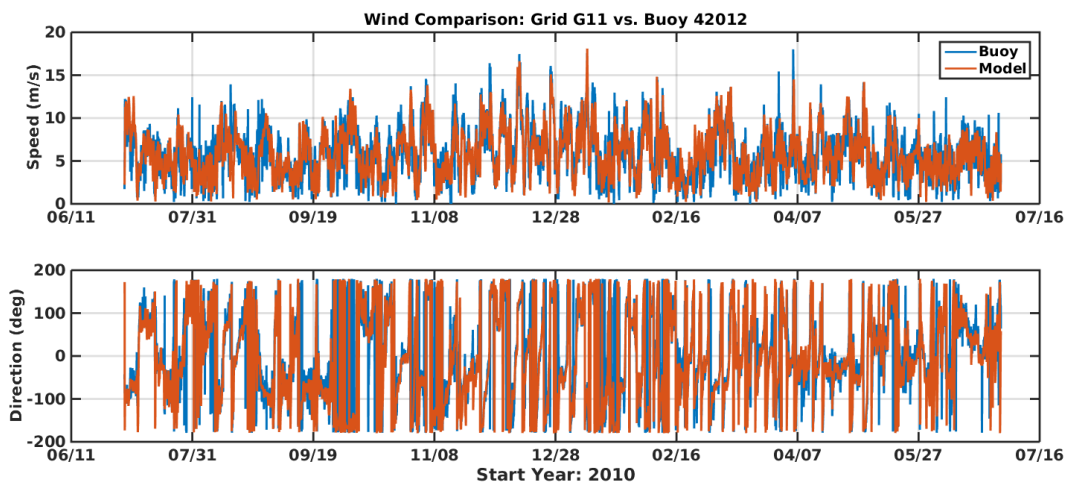


**Figure 6. Comparison of wind data (blue) and wind input (red) for the Gulf of Mexico test case. Wind speed (top) and direction (bottom) are shown for the location of Buoy 42012.**

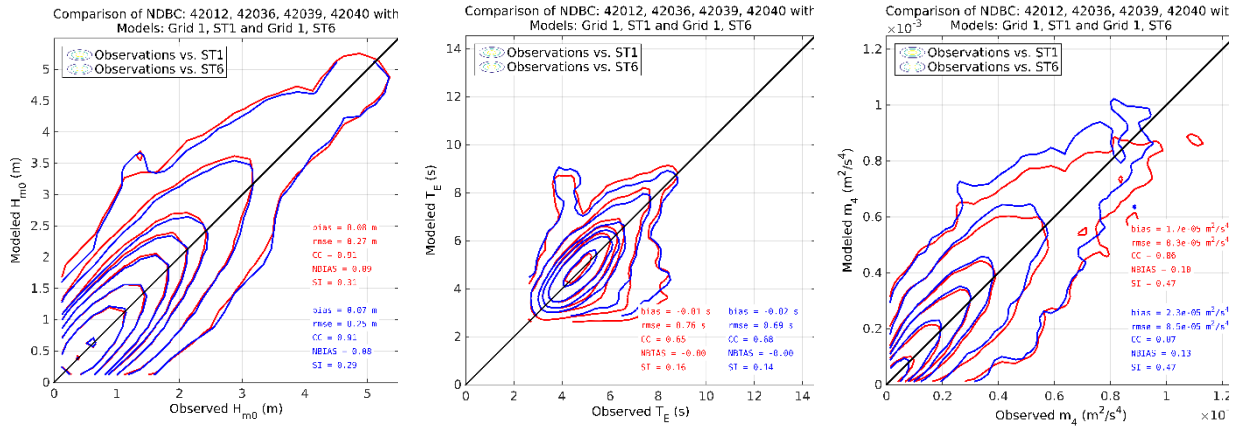


**Figure 7. Regression analysis of significant wave height (left), mean energy period (middle), 4th moment (right) using the ST1 package (red) and the ST6 package (blue) for the Gulf of Mexico G1 model.**

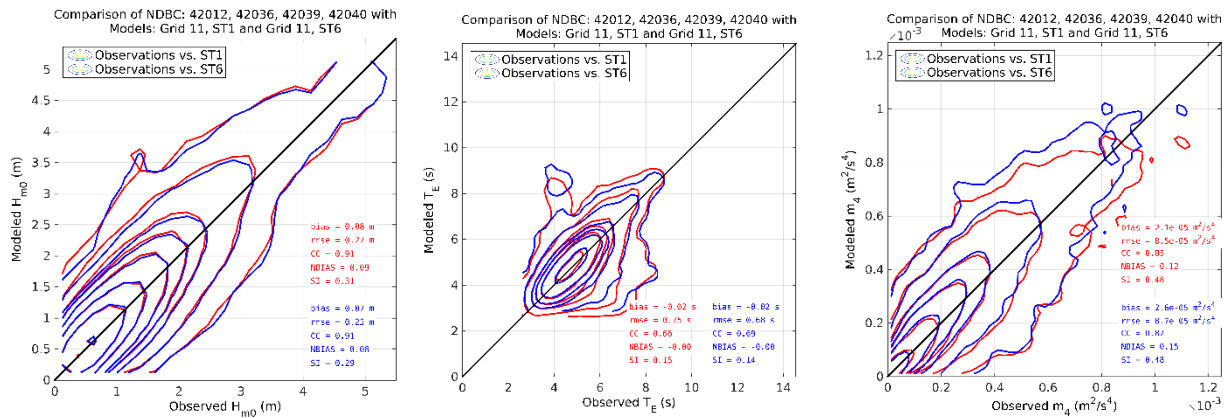


**Figure 8. Regression analysis of significant wave height (left), mean energy period (middle), 4th moment (right) using the ST1 package (red) and the ST6 package (blue) for the Gulf of Mexico G11 model.**

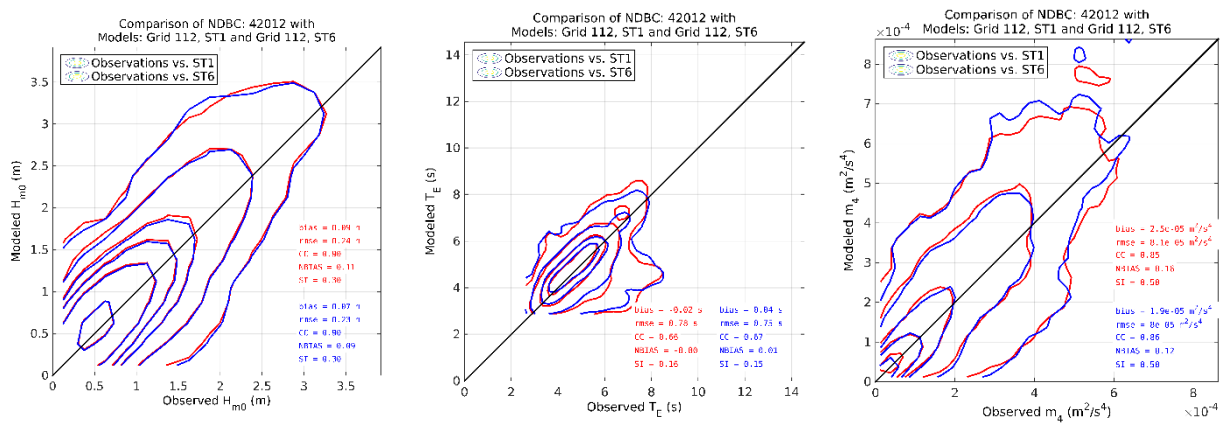


**Figure 9. Regression analysis of significant wave height (left), mean energy period (middle), 4th moment (right) using the ST1 package (red) and the ST6 package (blue) for the Gulf of Mexico G112 model.**

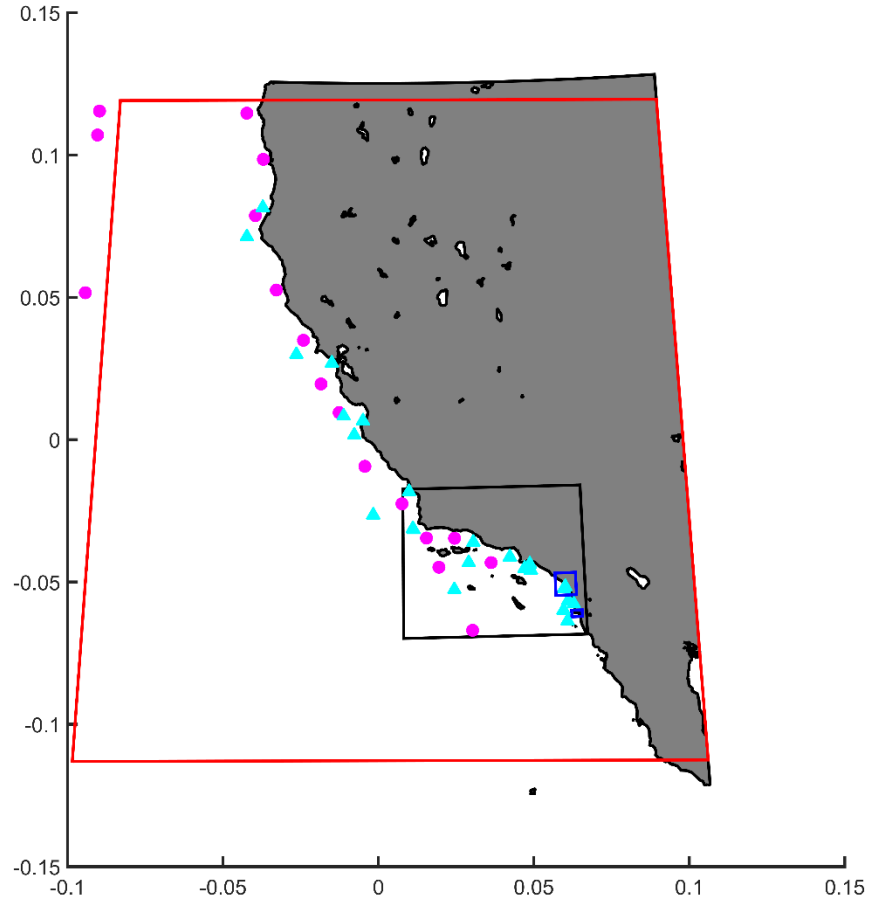


**Figure 10. Model grid configuration for the Southern California test case, Cal1 (red), Cal2 (black), Cal3 (blue) and NDBC (magenta circles) and Datawell (cyan triangles) buoys.**

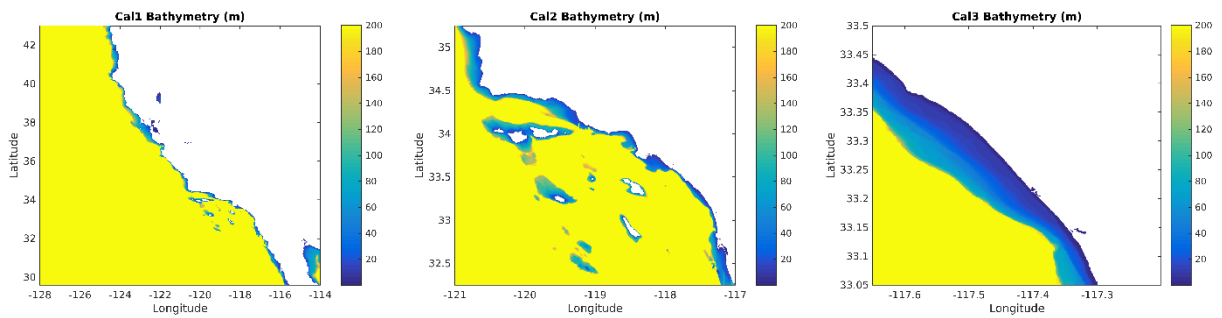


**Figure 11. Bathymetry Surfaces for Southern California Models, Cal1 (left), Cal2 (middle), Cal3 (right).**

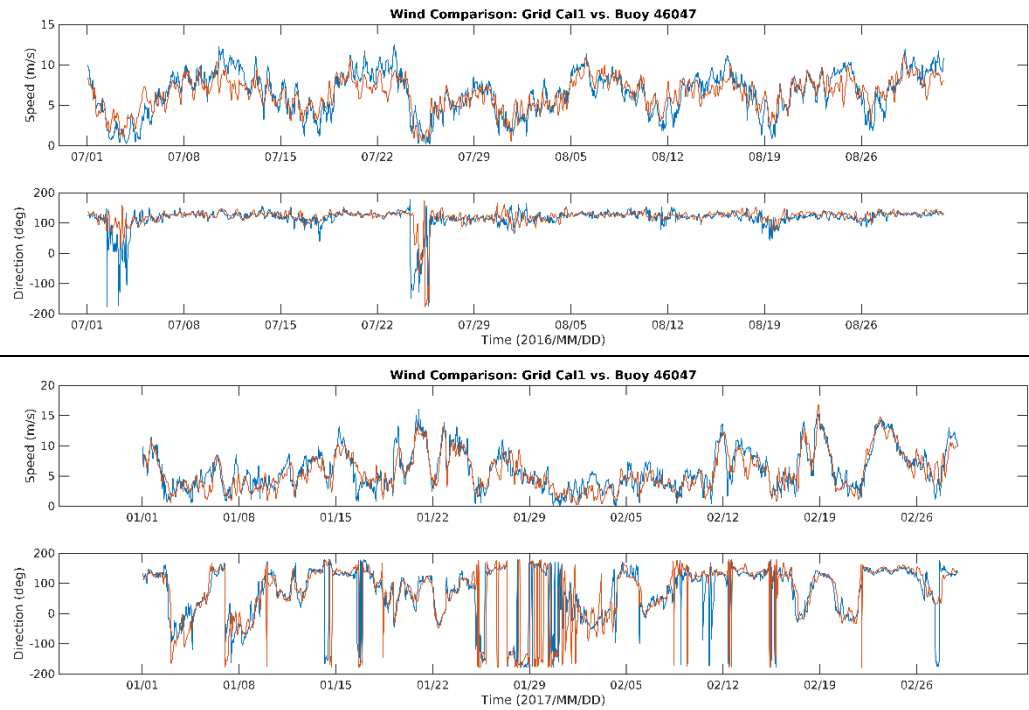


**Figure 12. Input (red) wind speed (top plot) and direction (bottom plot) compared to observations at NDBC Buoy 46047 (blue) for the summer (top half) and winter (bottom half) Southern California simulations.**

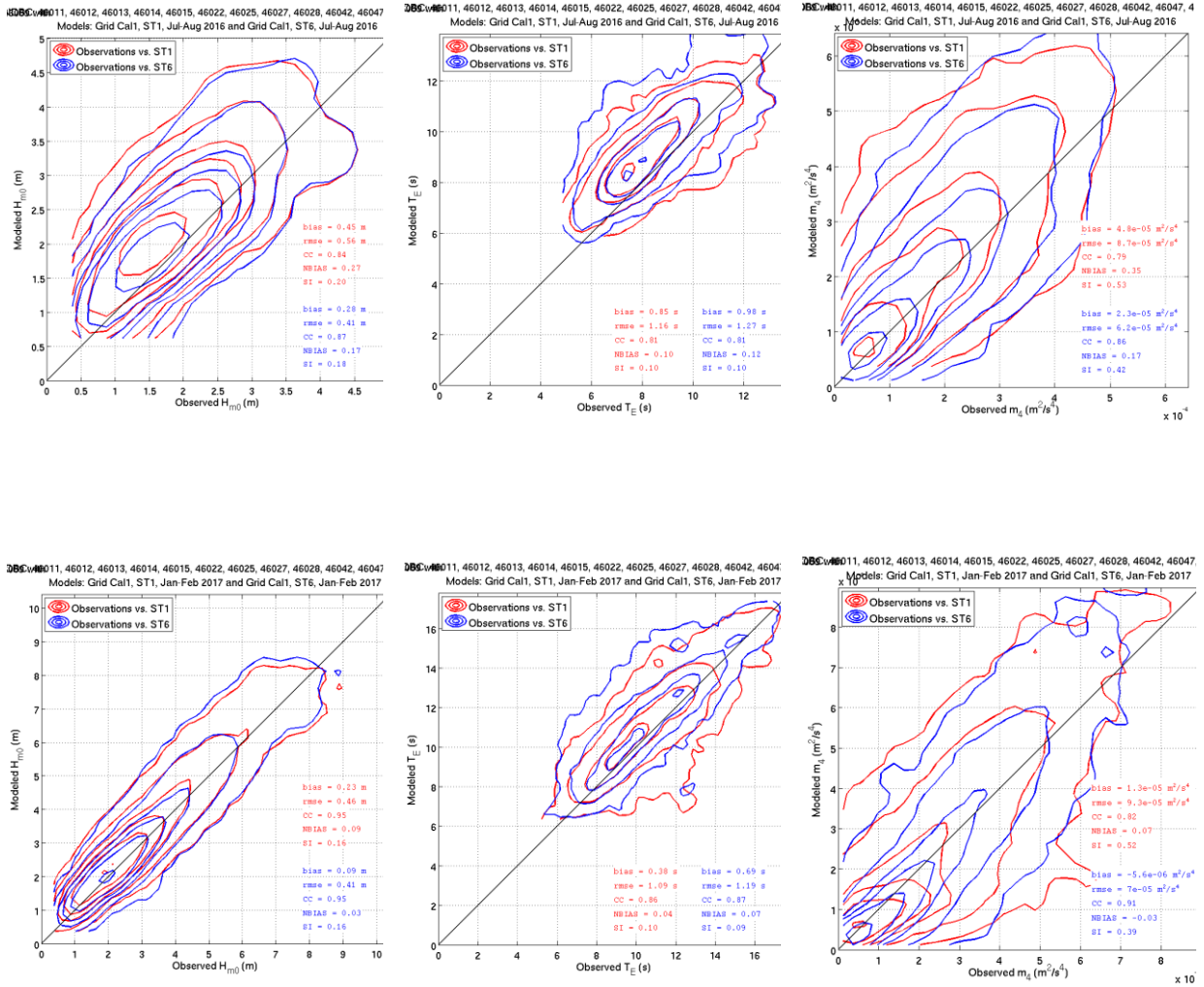


**Figure 13. Regression analysis of significant wave height (left), mean energy period (middle), 4th moment (right) using the ST1 package (red) and the ST6 package (blue) for the Southern California Call1 model and NDBC Buoys for the summer (top) and winter (bottom) periods.**

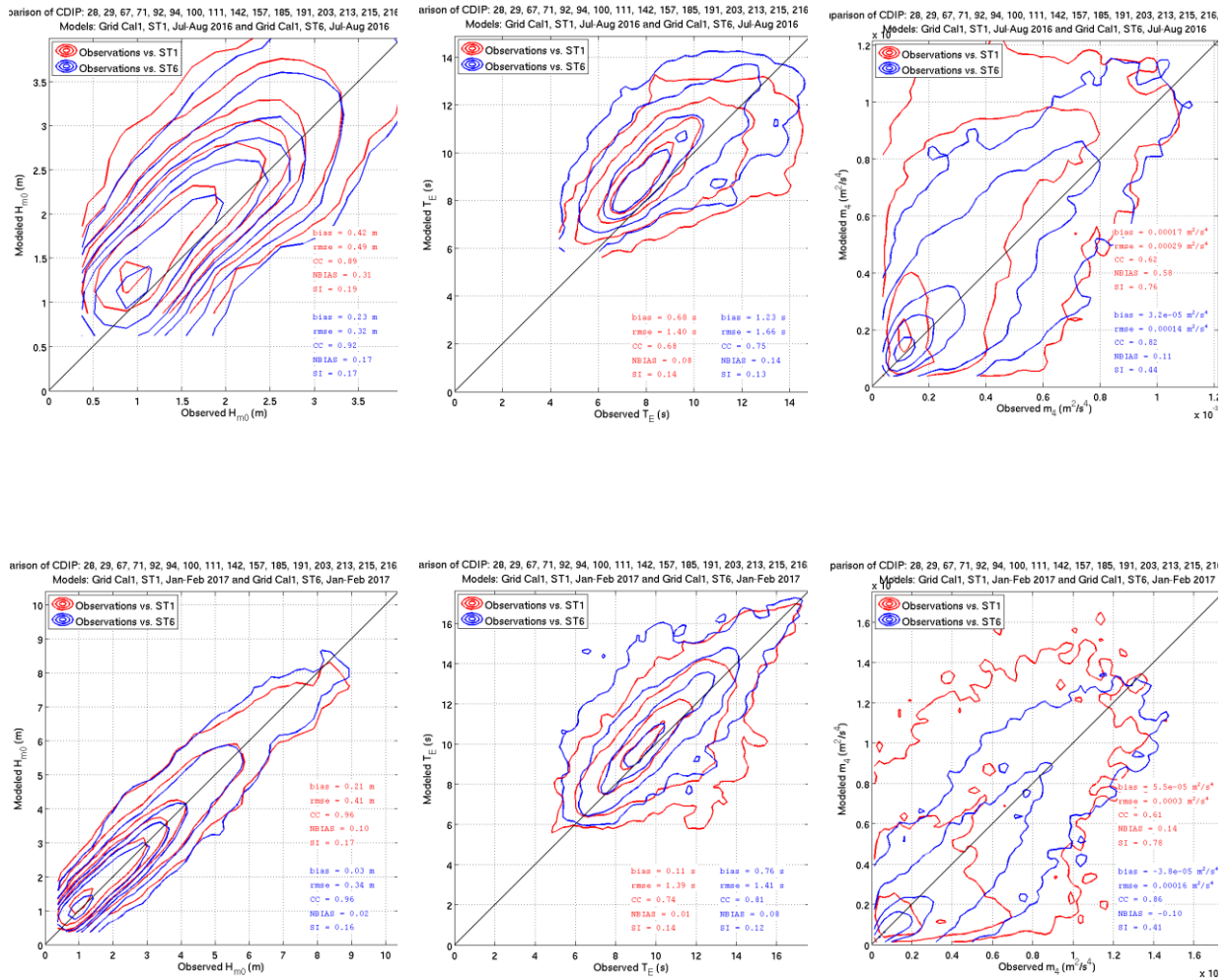


**Figure 14. Regression analysis of significant wave height (left), mean energy period (middle), 4th moment (right) using the ST1 package (red) and the ST6 package (blue) for the Southern California Cal1 model and Datawell Buoys for the summer (top) and winter (bottom) periods.**

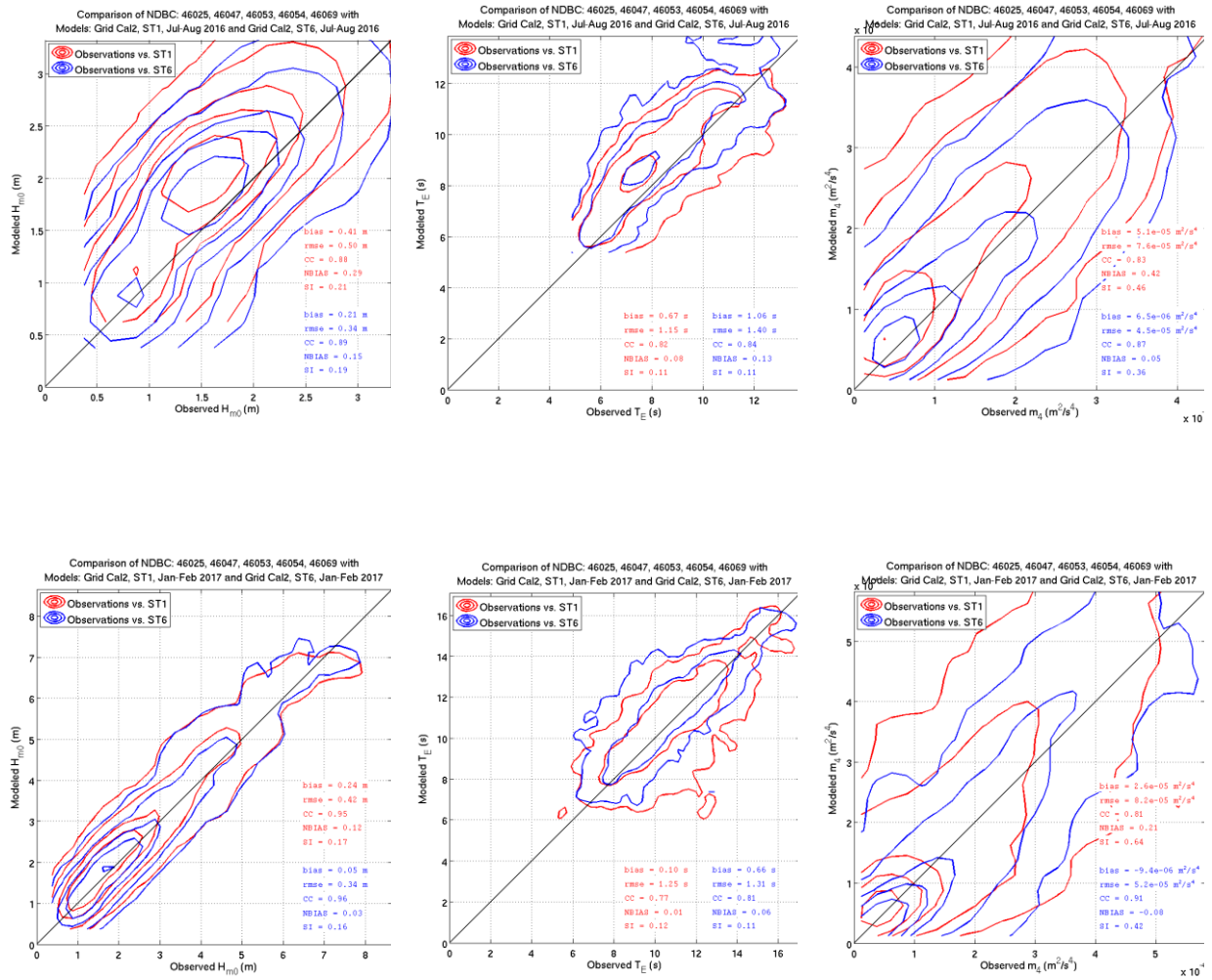


**Figure 15. Regression analysis of significant wave height (left), mean energy period (middle), 4th moment (right) using the ST1 package (red) and the ST6 package (blue) for the Southern California Cal2 model and NDBC Buoys for summer (top) and winter (bottom) periods.**

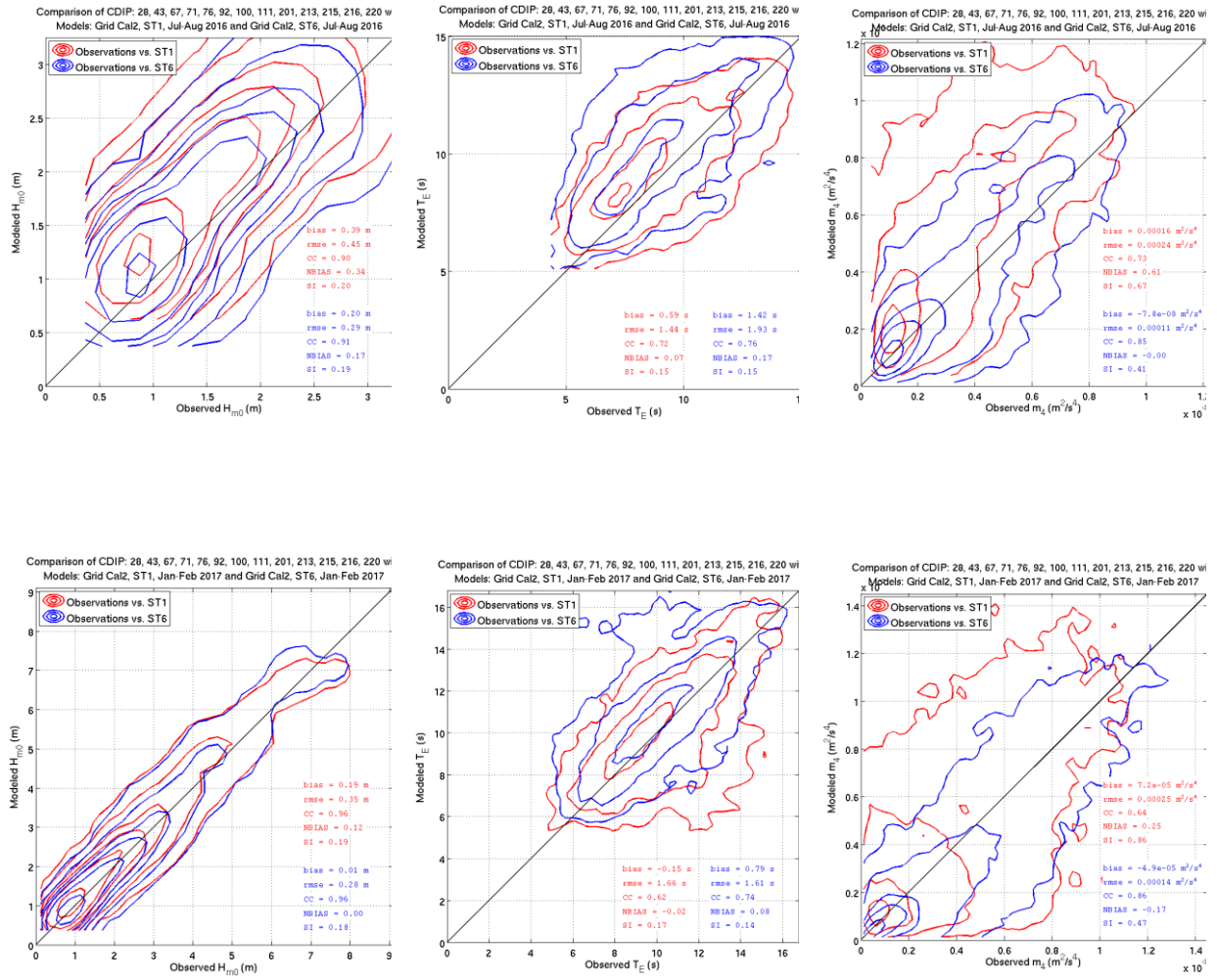


**Figure 16. Regression analysis of significant wave height (left), mean energy period (middle), 4th moment (right) using the ST1 package (red) and the ST6 package (blue) for the Southern California Cal2 model and Datawell Buoys for summer (top) and winter (bottom) periods.**

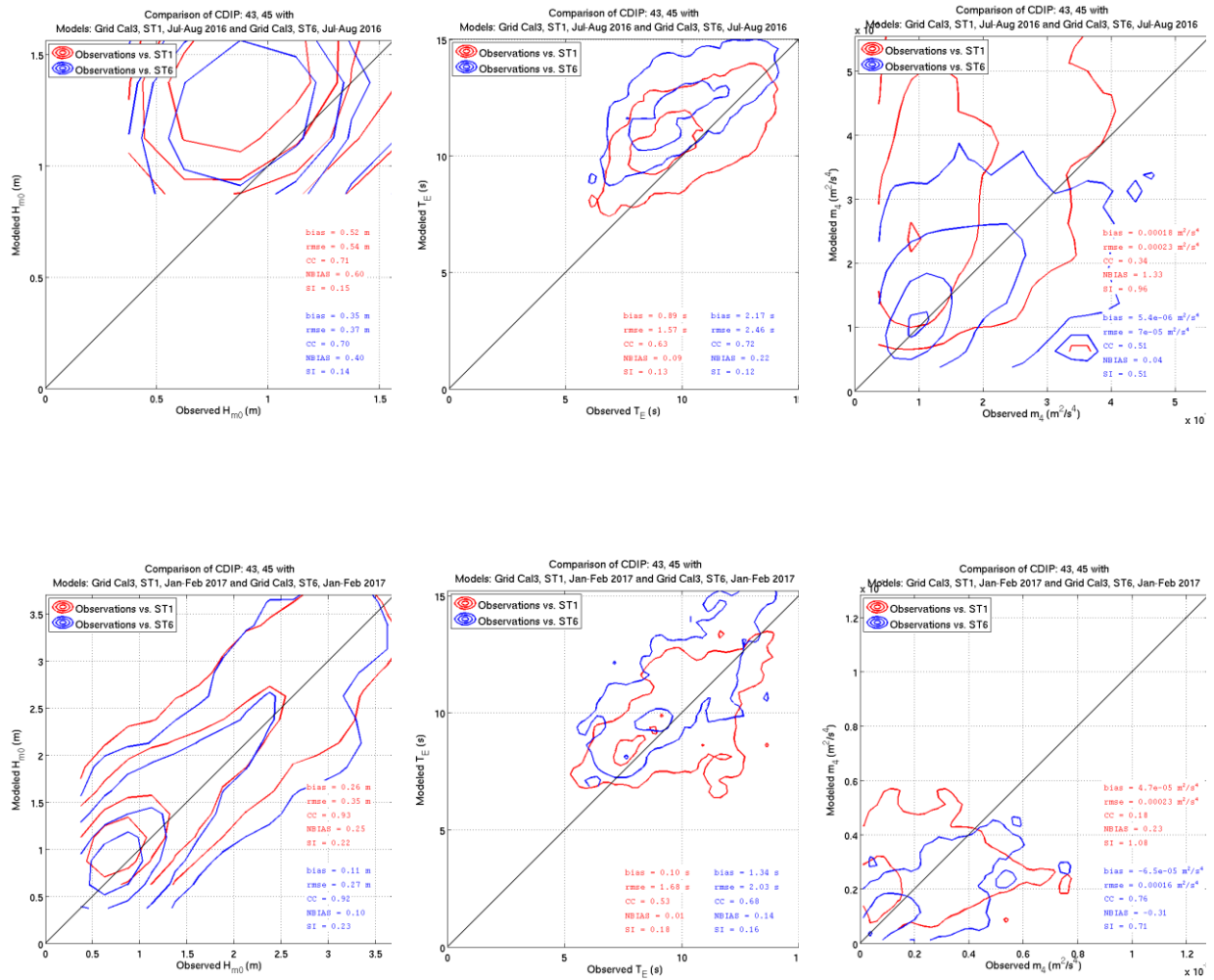


**Figure 17. Regression analysis of significant wave height (left), mean energy period (middle), 4th moment (right) using the ST1 package (red) and the ST6 package (blue) for Southern California Cal3 model and Datawell Buoys for summer (top) and winter (bottom) periods.**

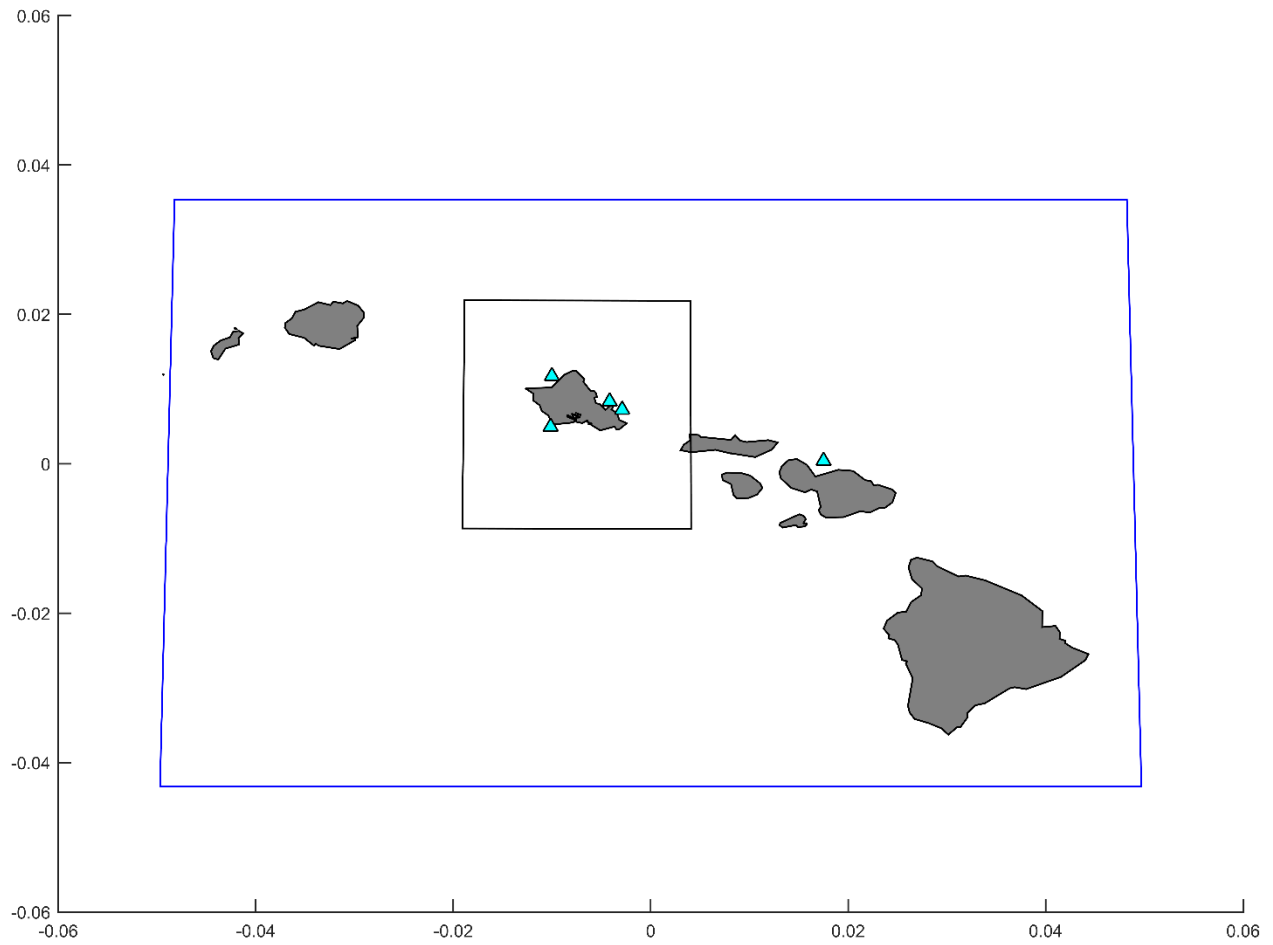


**Figure 18. Model grid configuration for the Hawaii test case, H1 (blue) and H2 (black) and Datawell Buoys (cyan triangles).**

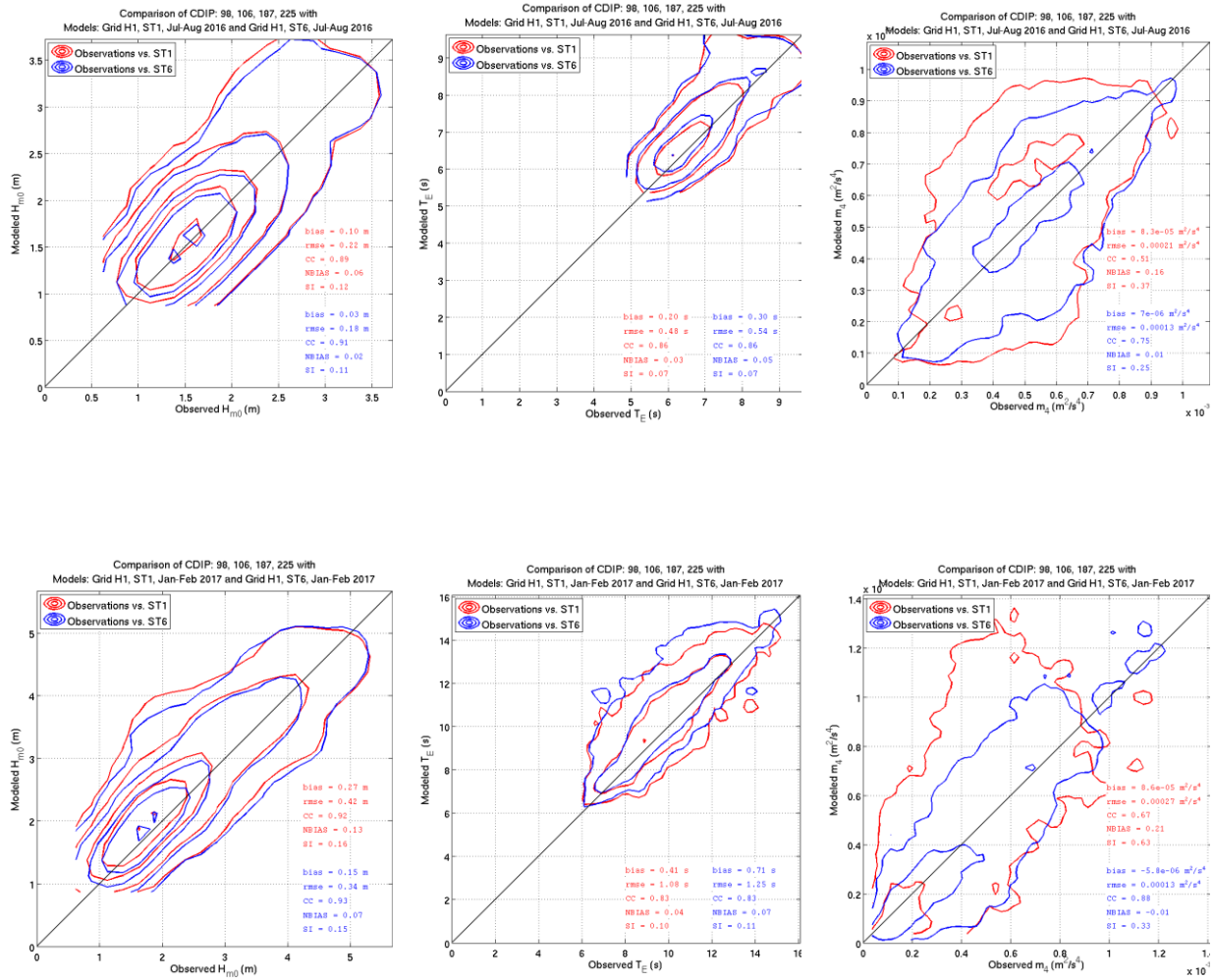


**Figure 19. Regression analysis of significant wave height (left), mean energy period (middle), 4th moment (right) using the ST1 package (red) and the ST6 package (blue) for the Hawaii H1 model and Datawell Buoys for summer (top) and winter (bottom) periods.**

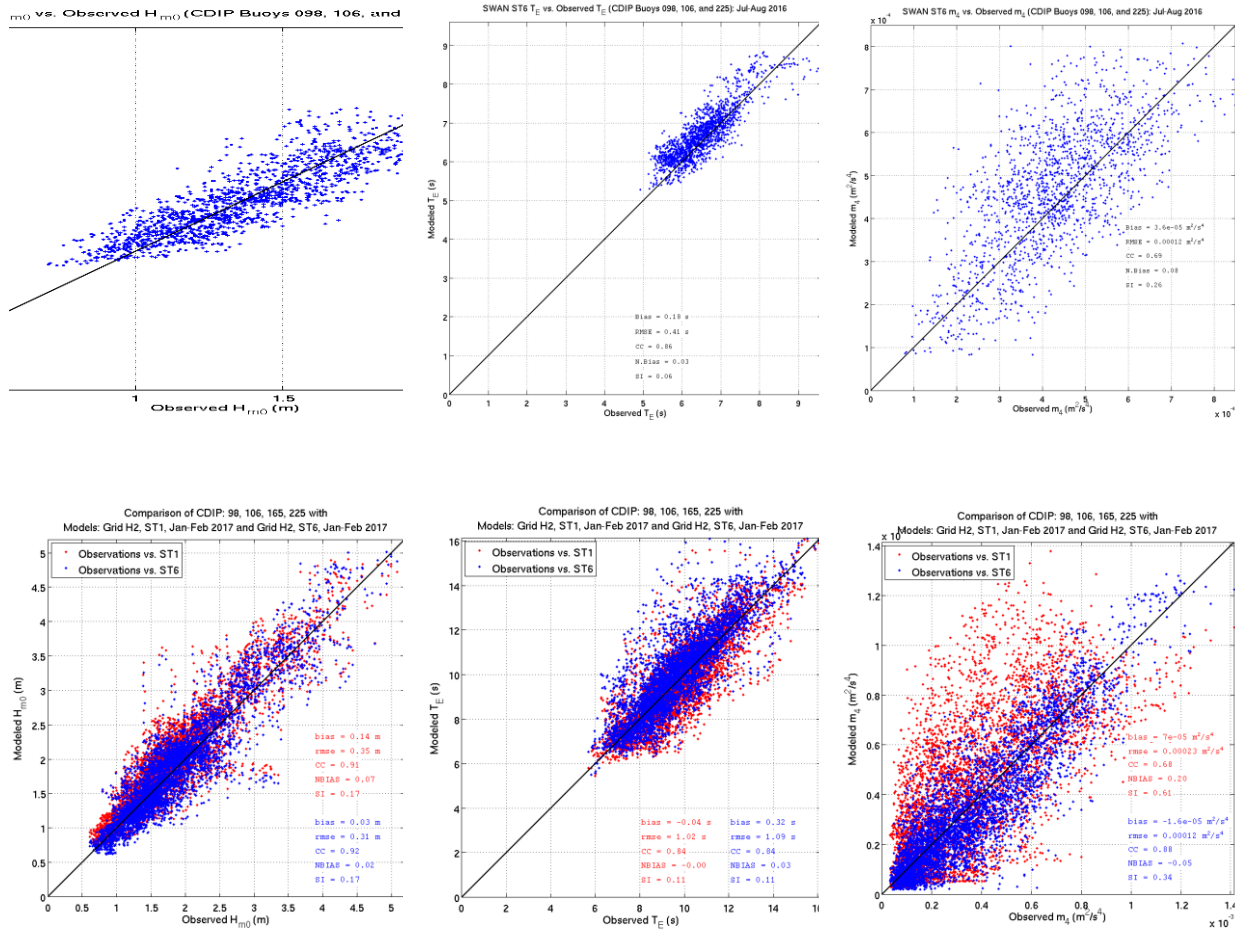


**Figure 20. Regression analysis of significant wave height (left), mean energy period (middle), 4th moment (right) using the ST1 package (red) and the ST6 package (blue) for the Hawaii H2 model and Datawell Buoys for summer (top) and winter (bottom) periods.**